

## Supplementary Information

# Modulating the DNA Cleavage Ability of Copper(II) Schiff Bases Through Ternary Complex Formation

*Joaquín Viqueira,<sup>a</sup> María L. Durán,<sup>a\*</sup> José A. García-Vázquez,<sup>a\*</sup>, Jesús Castro,<sup>b</sup> Carlos Platas-Iglesias,<sup>c</sup> David Esteban-Gómez,<sup>c</sup> Gloria Alzuet-Piña,<sup>d</sup> Angeles Moldes,<sup>d</sup> Otaciro R. Nascimento<sup>e</sup>*

<sup>a</sup>Departamento de Química Inorgánica, Campus Vida, Universidad de Santiago de Compostela, 15782 Santiago de Compostela (Galicia), Spain

<sup>b</sup>Departamento de Química Inorgánica, Facultade de Química, Edificio de Ciencias Experimentais, Universidade de Vigo, 36310 Vigo (Galicia), Spain

<sup>c</sup>Centro de Investigacións Científicas Avanzadas (CICA) and Departamento de Química, Universidade da Coruña, Campus da Zapateira, 15008 A Coruña (Galicia), Spain

<sup>d</sup>Departament de Química Inorgànica, Facultat de Farmàcia, Universitat de València, Avda. Vicent Andrés Estellés s/n, 46100 Burjassot (Valencia), Spain

<sup>e</sup>Instituto de Física de São Carlos, Universidade de São Paulo, CP 369, 13560-250 São Carlos, SP, Brazil

## Content

<b>Figure S1.</b> Superposition of the molecules <b>1</b> to show the different arrangement of the tolyl group: in orange <b>1a</b> and in green <b>1b</b> .....	5
<b>Figure S2.</b> Intramolecular and intermolecular $\pi$ - $\pi$ stacking interactions in <b>4</b> .....	6
<b>Figure S3.</b> EPR spectra of the mononuclear $[\text{CuL}^1(\text{phen})]$ ( <b>4</b> ) and $[\text{CuL}^2(2,2'\text{-bpy})]$ ( <b>6</b> ) complexes at powder and acetonitrile solutions. Spectral simulations are represented by thin lines over each experimental lines.....	7
<b>Figure S4.</b> Contour plots of the electron density (0.02 e Bohr <sup>-3</sup> ) of the $\beta$ LUMOs calculated for $[\text{CuL}^1(\text{H}_2\text{O})]$ (top) and $[\text{CuL}^1(2,2'\text{-bpy})]$ (bottom) .....	8
<b>Table S1.</b> Summary of crystal data and structure refinement .....	9
<b>Table S1 (cont)</b> Summary of crystal data and structure refinement .....	10
<b>Table S1 (cont)</b> Summary of crystal data and structure refinement .....	11
<b>Crystal structure of the ligand <math>[\text{H}_2\text{L}^1]\cdot\text{H}_2\text{O}</math></b> .....	12
<b>Figure S5.</b> ORTEP diagram of the molecular structure of $\text{H}_2\text{L}^1$ (mol. B). ....	12
<b>Table S2.</b> Selected Bond Distances (Å) and angles (°) for $\text{H}_2\text{L}^1$ .....	13
<b>Crystal packing of the compounds <b>1</b>, <b>3</b>, <b>4</b>, <b>6</b>, <b>7</b></b> .....	14
<b>Figure S6.</b> ORTEP diagram of the molecular structure of orthorhombic $[\text{CuL}^1(\text{H}_2\text{O})]\cdot\text{H}_2\text{O}$ ( <b>1b</b> ) showing intra and intermolecular hydrogen bonds .....	14
<b>Figure S7.</b> The Cu...O interactions in <b>1a</b> generate chains of complexes parallel to the crystallographic <i>a</i> axis. ....	15
<b>Table S3.</b> Hydrogen bonds and C-H... $\pi$ interactions for <b>1a</b> and <b>1b</b> [Å and °] .....	16
<b>Figure S8.</b> Growing along <i>b</i> axis for <b>1a</b> , see parameters in <b>Table S3</b> above .....	17
<b>Figure S9.</b> Crystal packing diagram for <b>1b</b> showing the interactions H...OH .....	17
<b>Figure S10.</b> View of the molecule <b>3</b> throw the 4,4'-bpy plane .....	18
<b>Table S4.</b> Parameters of the $\pi,\pi$ -stacking interactions for $[\text{Cu}_2\text{L}^1_2(4,4'\text{-bpy})]$ ( <b>3</b> ) .....	19
<b>Figure S11.</b> Crystal packing diagram of <b>3</b> showing $\pi,\pi$ -stacking interactions. ....	19
<b>Table S5.</b> Hydrogen bond parameters for $[\text{Cu}_2\text{L}^1_2(4,4'\text{-bpy})]$ ( <b>3</b> ) [Å and °] .....	19
<b>Figure S12.</b> Crystal packing diagram of <b>3</b> showing some as C-H...O interactions .....	20
<b>Table S6.</b> Parameters of the hydrogen bonds in $[\text{CuL}^1(\text{phen})]$ ( <b>4</b> ) .....	21
<b>Figure S13.</b> Intermolecular C-H...O interactions in <b>4</b> .....	21
<b>Table S7.</b> Parameters of the $\pi,\pi$ -stacking interactions in $[\text{CuL}^1(\text{phen})]$ ( <b>4</b> ).....	21
<b>Scheme S1.</b> Overlap along the <i>b</i> axis of the bpy rings of two neighboring molecules of <b>6</b> .....	22

<b>Table S8.</b> Hydrogen bonds for $[\text{CuL}^2(2,2'\text{-bpy})]$ ( <b>6</b> ) [Å and °] .....	23
<b>Table S9.</b> Parameters of the $\pi$ -stacking interactions for $[\text{CuL}^2(2,2'\text{-bpy})]$ ( <b>6</b> ).....	23
<b>Figure S14.</b> ORTEP view of <b>6</b> showing the $\pi,\pi$ -staking and some C-H···X (X = N, O) interactions.....	23
<b>Table S10.</b> Parameters of the $\pi,\pi$ -stacking interactions for ( <b>7</b> ).....	24
<b>Figure S15.</b> Crystal packing diagram of <b>7</b> showing $\pi,\pi$ -stacking interactions and a C-H···N interaction .....	25
<b>Table S11.</b> Hydrogen bonds parameters for $[\text{Cu}_2\text{L}^2_2(4,4'\text{-bpy})_3]$ ( <b>7</b> ) [Å and °].....	26
<b>Figure S16.</b> C-H···O interactions in <b>7</b> . Only two half of molecules were drawn in the sake of clarity. ....	26
<b>Hirshfeld surface analysis.</b> .....	27
<b>Figure S17.</b> View of $d_{\text{norm}}$ Hirschfeld surface analysis for one of the molecules found in the asymmetric unit of $\text{H}_2\text{L}^1 \cdot \text{H}_2\text{O}$ . (see text, molecule labeled as 1x) .....	28
<b>Figure S18.</b> View of $d_{\text{norm}}$ Hirschfeld surface analysis for one of the molecules found in the asymmetric unit of $\text{H}_2\text{L}^1 \cdot \text{H}_2\text{O}$ . This is for the molecule labeled as 2x.....	28
<b>Figure S19.</b> View of curvedness surface for one of the molecules found in the asymmetric unit of $\text{H}_2\text{L}^1 \cdot \text{H}_2\text{O}$ .....	29
<b>Figure S20.</b> View of <i>shape index</i> surface for the molecule labeled as 1x of $\text{H}_2\text{L}^1 \cdot \text{H}_2\text{O}$ .....	29
<b>Figure S21.</b> 2D fingerprint for $\text{H}_2\text{L}^1 \cdot \text{H}_2\text{O}$ .....	30
<b>Figure S22.</b> View of $d_{\text{norm}}$ Hirschfeld surface analysis for $[\text{CuL}^1(\text{H}_2\text{O})] \cdot \text{H}_2\text{O}$ ] ( <b>1a</b> ) .....	31
<b>Figure S23.</b> View of $d_{\text{norm}}$ Hirschfeld surface analysis for $[\text{CuL}^1(\text{H}_2\text{O})] \cdot \text{H}_2\text{O}$ ] ( <b>1b</b> ).....	31
<b>Figure S24.</b> View of curvedness surface for $[\text{CuL}^1(\text{H}_2\text{O})] \cdot \text{H}_2\text{O}$ ] ( <b>1a</b> ).....	31
<b>Figure S25.</b> View of <i>shape index</i> surface for $[\text{CuL}^1(\text{H}_2\text{O})] \cdot \text{H}_2\text{O}$ ] ( <b>1a</b> ).....	32
<b>Figure S26.</b> View of curvedness surface for $[\text{CuL}^1(\text{H}_2\text{O})] \cdot \text{H}_2\text{O}$ ] ( <b>1b</b> ).....	32
<b>Figure S27.</b> View of <i>shape index</i> surface for $[\text{CuL}^2(\text{H}_2\text{O})] \cdot \text{H}_2\text{O}$ ] ( <b>1b</b> ) .....	32
<b>Figure S28.</b> 2D fingerprint for $[\text{CuL}^1(\text{H}_2\text{O})] \cdot \text{H}_2\text{O}$ ], triclinic ( <b>1a</b> ).....	33
<b>Figure S29.</b> 2D fingerprint for for $[\text{CuL}^1(\text{H}_2\text{O})] \cdot \text{H}_2\text{O}$ ] orthorhombic ( <b>1b</b> ) .....	33
<b>Figure S30.</b> View of $d_{\text{norm}}$ Hirschfeld surface analysis for $[\text{Cu}_2\text{L}^1_2(4,4'\text{-bpy})]$ ( <b>3</b> ) .....	34
<b>Figure S31.</b> View of curvedness surface for $[\text{Cu}_2\text{L}^2_2(4,4'\text{-bpy})]$ ( <b>3</b> ) .....	34
<b>Figure S32.</b> View of <i>shape index</i> surface for $[\text{Cu}_2\text{L}^2_2(4,4'\text{-bpy})]$ ( <b>3</b> ) .....	35
<b>Figure S33.</b> 2D fingerprint for $[\text{Cu}_2\text{L}^1_2(4,4'\text{-bpy})]$ ( <b>3</b> ). .....	35
<b>Figure S34.</b> View of $d_{\text{norm}}$ Hirschfeld surface analysis for $[\text{CuL}^1(\text{phen})]$ ( <b>4</b> ).....	36

<b>Figure S35.</b> View of curvedness surface for [CuL <sup>1</sup> (phen)] ( <b>4</b> ).....	36
<b>Figure S36.</b> View of <i>shape index</i> surface for [CuL <sup>1</sup> (phen)] ( <b>4</b> ) .....	37
<b>Figure S37.</b> 2D fingerprint for [CuL <sup>1</sup> (phen)] ( <b>4</b> ).....	37
<b>Figure S38.</b> View of d <sub>norm</sub> Hirschfeld surface analysis for [CuL <sup>2</sup> (2,2'-bpy)] ( <b>6</b> ) .....	38
<b>Figure S39.</b> View of curvedness surface for [CuL <sup>2</sup> (2,2'-bpy)] ( <b>6</b> ) .....	38
<b>Figure S40.</b> View of <i>shape index</i> surface for [CuL <sup>2</sup> (2,2'-bpy)] ( <b>6</b> ). ....	39
<b>Figure S41.</b> 2D fingerprint for [CuL <sup>2</sup> (2,2'-bpy)] ( <b>6</b> ).....	39
<b>Figure S42.</b> View of d <sub>norm</sub> Hirschfeld surface analysis for [Cu <sub>2</sub> L <sup>2</sup> <sub>2</sub> (4,4'-bpy) <sub>3</sub> ] ( <b>7</b> ) .....	40
<b>Figure S43.</b> View of curvedness surface for [Cu <sub>2</sub> L <sup>1</sup> <sub>2</sub> (4,4'-bpy) <sub>3</sub> ] ( <b>7</b> ).....	41
<b>Figure S44.</b> View of <i>shape index</i> surface for [Cu <sub>2</sub> L <sup>1</sup> <sub>2</sub> (4,4'-bpy) <sub>3</sub> ] ( <b>7</b> ). ....	41
<b>Figure S45.</b> 2D fingerprint for for [Cu <sub>2</sub> L <sup>2</sup> <sub>2</sub> (4,4'-bpy) <sub>3</sub> ] ( <b>7</b> ). ....	42
<b>DFT calculations</b> .....	43
<b>Table S12.</b> Selected Bond Lengths (Å) and angles (°) for the triclinic ( <b>1a</b> ) and orthorhombic ( <b>1b</b> ) forms of [CuL <sup>1</sup> (H <sub>2</sub> O)]·H <sub>2</sub> O and the DFT calculated geometry .....	42
<b>Table S13.</b> Selected Bond Lengths (Å) and angles (°) for <b>4</b> and <b>6</b> complexes and corresponding calculated geometries.....	43
<b>Table S14.</b> Optimized Cartesian coordinates (Å) for [CuL <sup>1</sup> (H <sub>2</sub> O)]·H <sub>2</sub> O .....	44
<b>Table S15.</b> Optimized Cartesian coordinates (Å) for [CuL <sup>2</sup> (2,2'-bpy)].....	45
<b>Table S16.</b> Optimized Cartesian coordinates (Å) for [CuL <sup>1</sup> (phen)]. .....	47
<b>Table S17.</b> Optimized Cartesian coordinates (Å) for [CuL <sup>1</sup> (4,4'-bpy)]. .....	49
<b>Table S18.</b> Optimized Cartesian coordinates (Å) for [CuL <sup>1</sup> (4,4'-bpy) <sub>2</sub> ]. .....	51
<b>Table S19.</b> Optimized Cartesian coordinates (Å) for [CuL <sup>2</sup> (4,4'-bpy)]. .....	53
<b>Table S20.</b> Optimized Cartesian coordinates (Å) for [CuL <sup>2</sup> (4,4'-bpy) <sub>2</sub> ]. .....	55
<b>References</b> .....	57

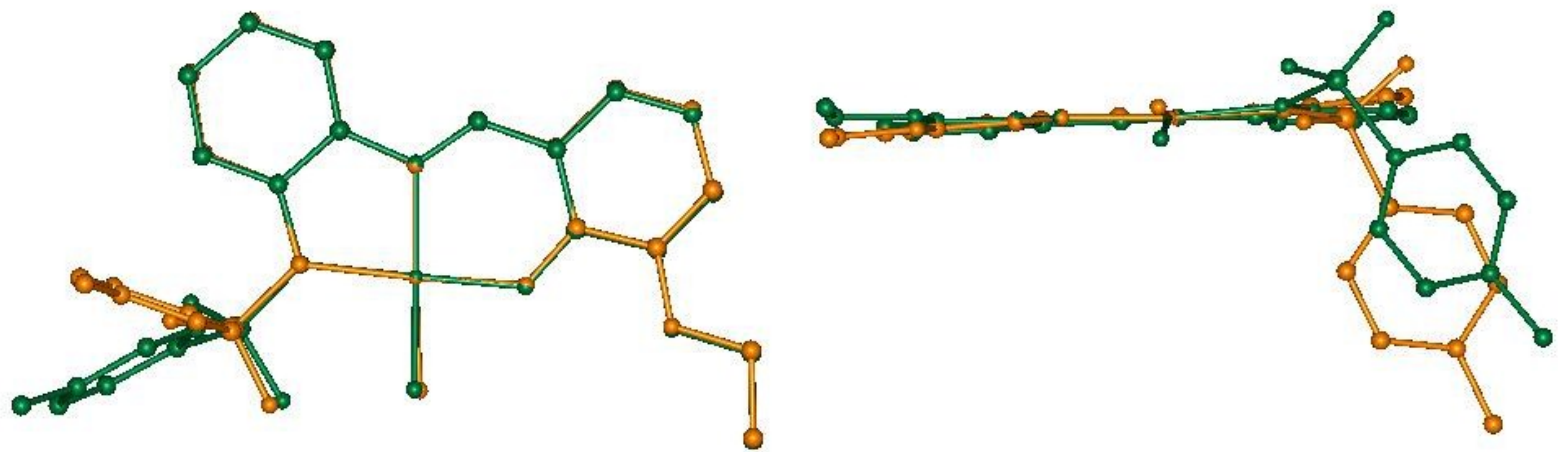


**Fig. S1** Superposition of the molecules **1** to show the different arrangement of the tolyl group: in orange **1a** and in green **1b**.

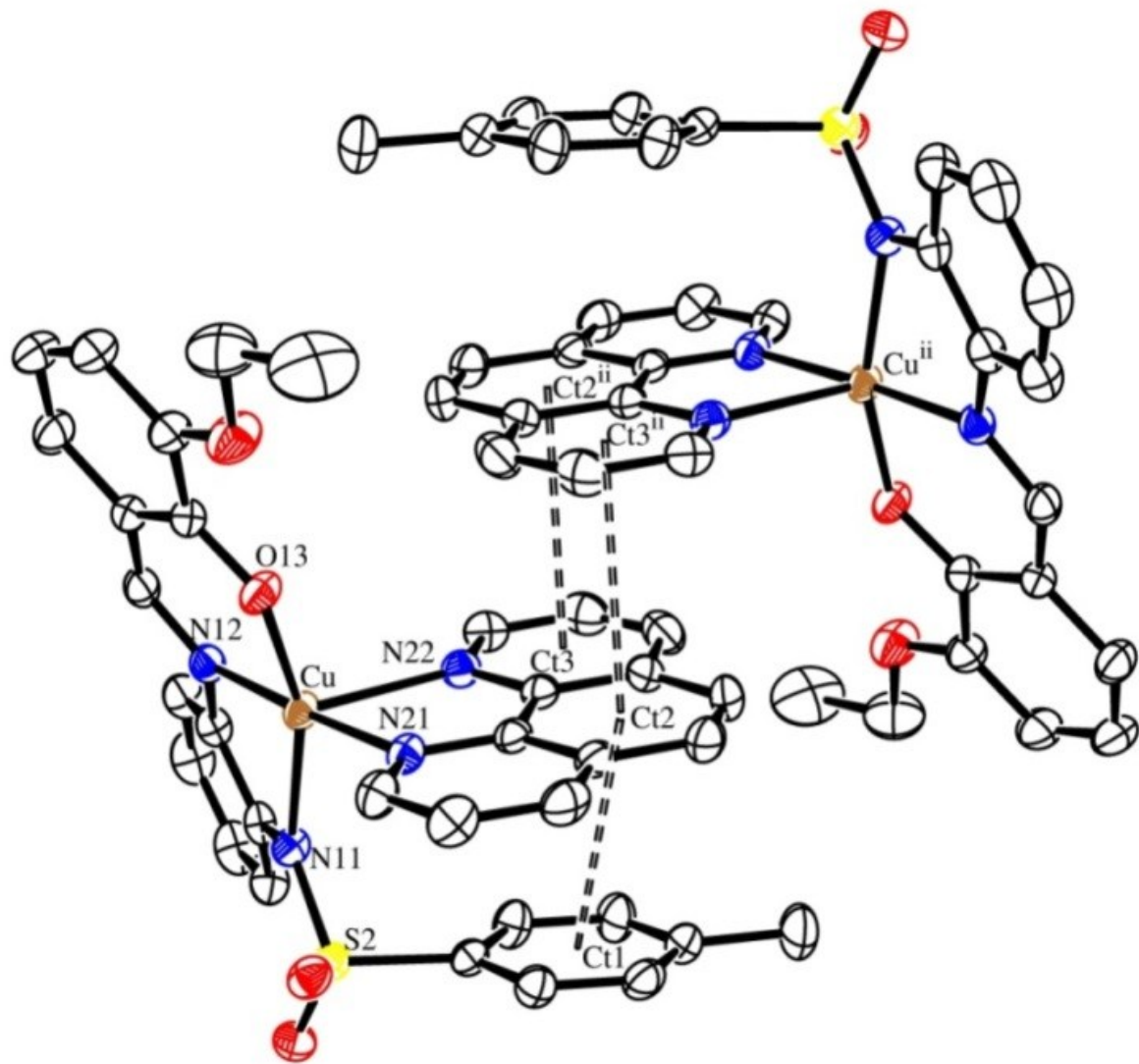


**Fig. S2** Intramolecular and intermolecular  $\pi$ - $\pi$  stacking interactions in **4**.

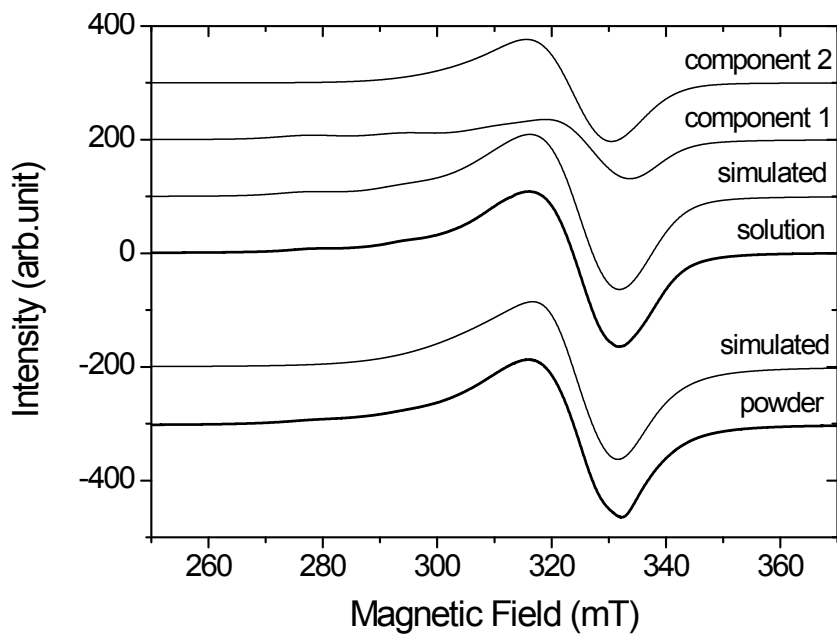
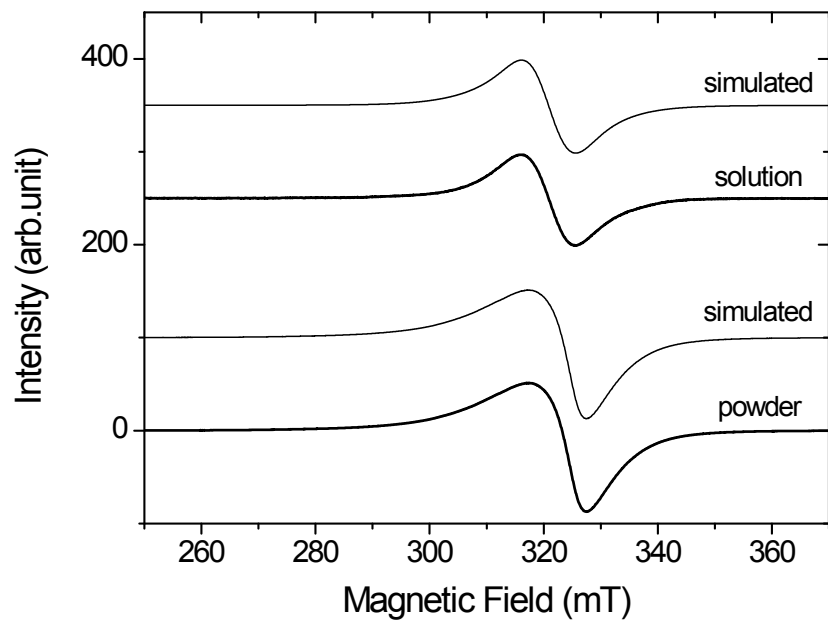


**Fig. S3** EPR spectra of the mononuclear  $[\text{CuL}^1(\text{phen})]$  (**4**) and  $[\text{CuL}^2(2,2'\text{-bpy})]$  (**6**) complexes at powder and acetonitrile solutions. Spectral simulations are represented by thin lines over each experimental lines.

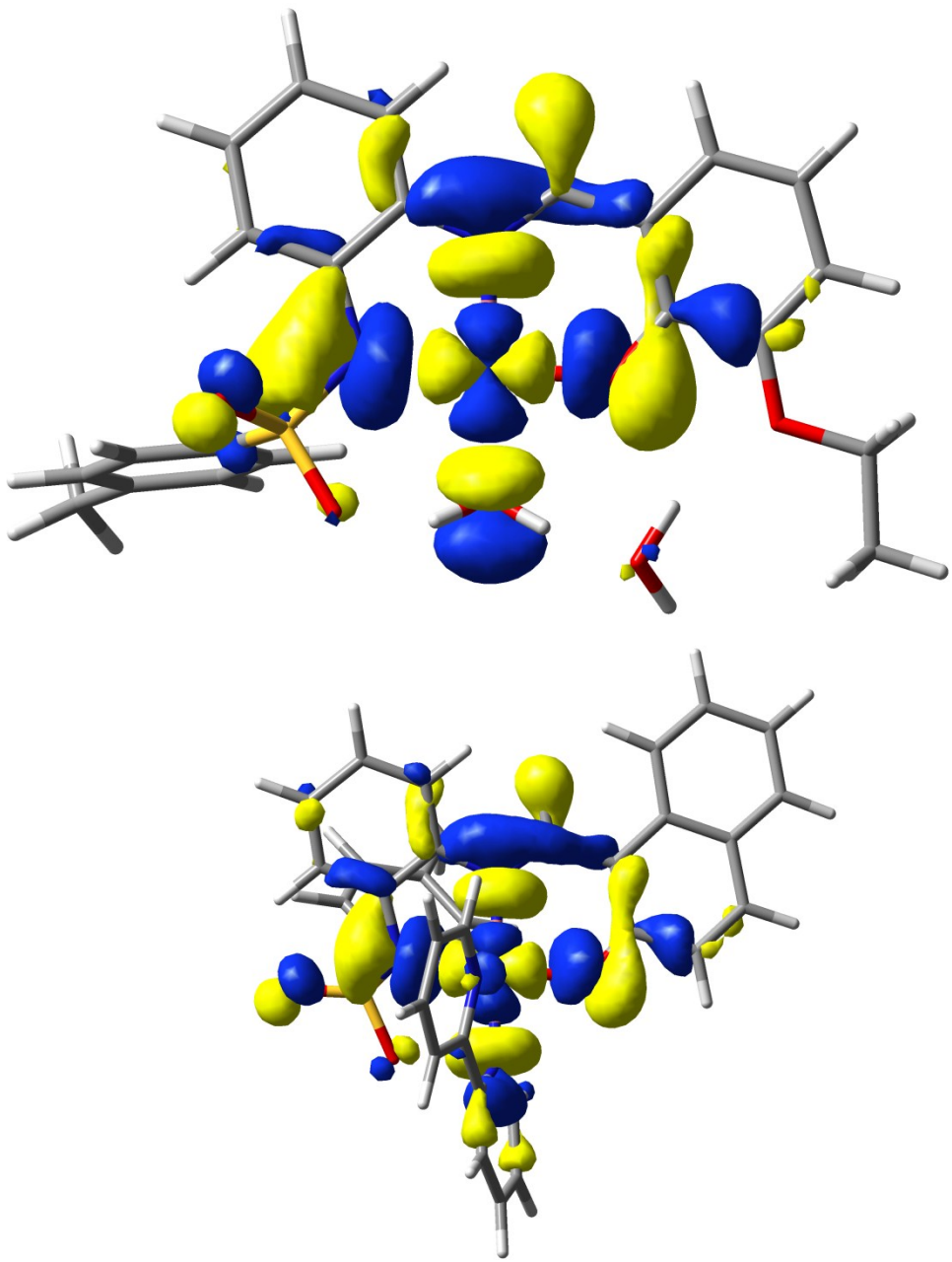


**Fig. S4** Contour plots of the electron density ( $0.02 \text{ e Bohr}^{-3}$ ) of the  $\beta$  LUMOs calculated for  $[\text{CuL}^1(\text{H}_2\text{O})]$  (top) and  $[\text{CuL}^1(2,2'\text{-bpy})]$  (bottom).

**Table S1.** Summary of crystal data and structure refinement.

Compound	H <sub>2</sub> L <sup>1</sup> ·H <sub>2</sub> O	[CuL <sup>1</sup> (H <sub>2</sub> O)]H <sub>2</sub> O ( <b>1a</b> )	[CuL <sup>1</sup> (H <sub>2</sub> O)]H <sub>2</sub> O ( <b>1b</b> )
Empirical formula	C <sub>22</sub> H <sub>23</sub> N <sub>2</sub> O <sub>5</sub> S	C <sub>22</sub> H <sub>24</sub> N <sub>2</sub> O <sub>6</sub> SCu	C <sub>22</sub> H <sub>24</sub> N <sub>2</sub> O <sub>6</sub> SCu
Formula weight	427.48	508.03	508.03
Crystal size, mm	0.60 x 0.60 x 0.35	0.31 x 0.28 x 0.08	0.52 x 0.24 x 0.13
Temperature, K	293(2)	293(2)	293(2)
Wavelength, Å	1.5418	0.71073	1.54180
Crystal system	Orthorhombic	Triclinic	Orthorhombic
Space group	Pna2 <sub>1</sub>	P-1	Pca2 <sub>1</sub>
Unit cell dimensions			
a, Å	11.646(13)	5.754(2)	22.663(4)
b, Å	9.278(16)	9.595(3)	10.1552(7)
c, Å	39.24(6)	19.723(7)	9.7130(6)
α/°	90	90.663(6)	90
β/°	90	91.571(6)	90
γ/°	90	100.876(6)	90
Volume, Å <sup>3</sup>	4240(11)	1068.8(6)	2235.4(4)
Z	8	2	4
μ, mm <sup>-1</sup>	1.339	1.163	1.510
No. reflections collected	4442	19778	2646
Data / restraints / parameters	4441 / 2 / 564	5307 / 0 / 306	2443 / 1 / 300
Goodness-of-fit	1.094	1.041	1.057
Absolute structure parameter	0.07(5)		-0.04(3)
Final R indices [I>2σ(I)]	<sup>a</sup> R <sub>1</sub> = 0.0782 <sup>b</sup> wR <sub>2</sub> = 0.2062	<sup>a</sup> R <sub>1</sub> = 0.0346 <sup>b</sup> wR <sub>2</sub> = 0.0817	<sup>a</sup> R <sub>1</sub> = 0.0334 <sup>b</sup> wR <sub>2</sub> = 0.0892

$$^a R_1 = \sum[|F_O| - |F_C|] / \sum|F_O|; ^b wR_2 = [(\sum(F_O^2 - F_C^2)) / \sum(F_O^2)]^{1/2}$$

**Table S1** (cont) Summary of crystal data and structure refinement.

Compound	[Cu <sub>2</sub> L <sup>1</sup> <sub>2</sub> (4,4'-bpy)] ( <b>3</b> )	[CuL <sup>1</sup> (phen)] ( <b>4</b> )
Empirical formula	C <sub>27</sub> H <sub>24</sub> N <sub>3</sub> O <sub>4</sub> SCu	C <sub>34</sub> H <sub>28</sub> N <sub>4</sub> O <sub>4</sub> SCu
Formula weight	550.09	652.20
Crystal size, mm	0.22 x 0.16 x 0.02	0.30 x 0.22 x 0.20 mm
Temperature, K	100(2)	293(2)
Wavelength, Å	0.71073	0.71073
Crystal system	Triclinic	Monoclinic
Space group	P-1	C2/c
Unit cell dimensions		
a, Å	9.1259(18)	24.6147(17)
b, Å	10.853(2)	12.9395(8))
c, Å	13.207(2)	21.9303(15)
α/°	101.339(11)	90(2)
β/°	100.351(10)	117.6430(10)
γ/°	110.211(10)	90(2)
Volume, Å <sup>3</sup>	1159.1(4) Å <sup>3</sup>	6187.6(7)
Z	2	8
μ, mm <sup>-1</sup>	1.074	0.818
No. reflections collected	20306	17494
Data / restraints / parameters	4535 / 0 / 327	7004 / 0/ 399
Goodness-of-fit	1.001	0.819
Final R indices [I>2σ(I)]	<sup>a</sup> R <sub>1</sub> = 0.0503 <sup>b</sup> wR <sub>2</sub> = 0.0999	<sup>a</sup> R <sub>1</sub> = 0.0455 <sup>b</sup> wR <sub>2</sub> = 0.0935

$$^a R_1 = \sum[|F_o| - |F_c|] / \sum |F_o|; ^b wR_2 = [\sum(F_o^2 - F_c^2) / \sum(F_o^2)]^{1/2}$$

**Table S1** (cont) Summary of crystal data and structure refinement.

Compound	[CuL <sup>2</sup> (2,2'-bpy)] ( <b>6</b> )	[Cu <sub>2</sub> L <sup>2</sup> (4,4'-bpy) <sub>3</sub> ] ( <b>7</b> )
Empirical formula	C <sub>34</sub> H <sub>26</sub> N <sub>4</sub> O <sub>3</sub> SCu	C <sub>39</sub> H <sub>30</sub> N <sub>5</sub> O <sub>3</sub> SCu
Formula weight	634.19	712.28
Crystal size, mm	0.30 x 0.26 x 0.10	0.47 x 0.40 x 0.07
Temperature, K	100(2)	293(2)
Wavelength, Å	0.71073	0.71073
Crystal system	Monoclinic	Triclinic
Space group	P2 <sub>1</sub> /c	P-1
Unit cell dimensions		
a, Å	10.0829(18)	9.203(3)
b, Å	16.324(3)	12.352(4)
c, Å	16.992(3)	15.197(5)
α/°	90	70.384(6)
β/°	97.003(3)	83.857(5)
γ/°	90	86.570(5)
Volume, Å <sup>3</sup>	2775.9(9)	1617.5(9)
Z	4	2
μ, mm <sup>-1</sup>	0.907	0.788
No. reflections collected	25540	29072
Data / restraints / parameters	6118 / 0 / 389	7401 / 0 / 443
Goodness-of-fit	1.060	1.039
Final R indices [I>2σ(I)]	<sup>a</sup> R <sub>1</sub> = 0.0358 <sup>b</sup> wR <sub>2</sub> = 0.0781	<sup>a</sup> R <sub>1</sub> = 0.0366 <sup>b</sup> wR <sub>2</sub> = 0.0844

$$^a R_1 = \sum[|F_o| - |F_c|] / \sum |F_o|; ^b wR_2 = [\sum(F_o^2 - F_c^2) / \sum(F_o^2)]^{1/2}$$

### Crystal structure of the ligand $[H_2L^1] \cdot H_2O$ .

The asymmetric unit contains two independent molecules that are chemically similar and two molecules of water. For the sake of clarity, only one of these molecules is shown in Figure 1 (main text), and the other one is shown at Figure S5, both with the atomic numbering scheme adopted. A selection of bond lengths and angles for  $[H_2L^1] \cdot H_2O$  are in Table S2.

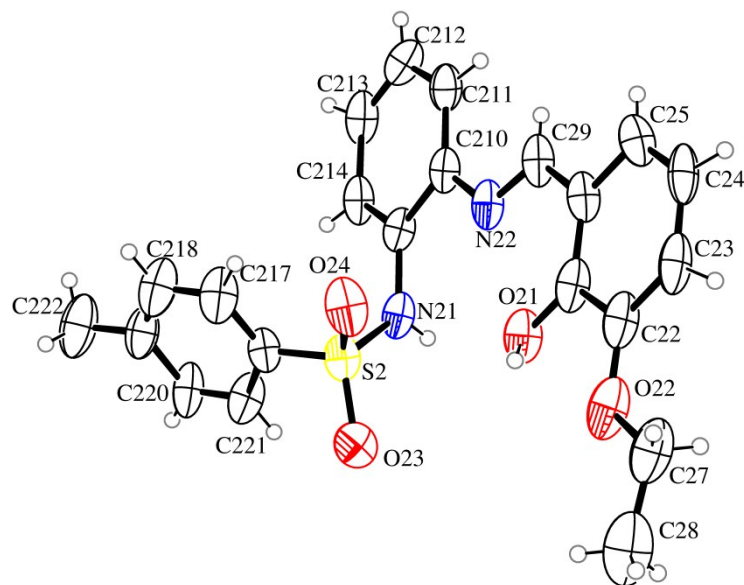


**Fig. S5** ORTEP diagram of the molecular structure of  $H_2L^1$  (mol. B).

The most noticeable structural parameters in the ligand are the relatively short value for the bond distance of the imino group [N(12)-C(19) 1.317(11) Å in molecule A and N(22)-C(29) 1.277(12) Å in molecule B respectively]. Both values are consistent with the existence of a double bond between these atoms.<sup>1</sup> The values of the other C-N bond distances [1.434(10) Å in molecule A and 1.397(11) Å in molecule B] correspond to a single bond between carbon and nitrogen atoms. Similarly, bond distances involving the ring and the oxygen atom from the ethoxy group [1.377(13) and 1.354(13) Å, respectively in both molecules] are consistent with a single bond C–O.<sup>2-5</sup> However the values for the bond distances between the carbon atom and the

phenolic oxygen atom [C(11)-O(11) 1.311(10) and C(21)-O(21) 1.295(11) Å for respectively both molecules] are shorter than the mentioned above and those found in other organic ligands containing phenolic fragments [in the range 1.343 to 1.353 Å].<sup>3-5</sup> Remaining bond distances and angles in the ligand are similar to those found in other Schiff base ligands and do not deserve additional discussion.

It is worth noting that, excluding the tosyl group, the remaining ligand adopts a planar disposition [maximum deviation of 0.0886 Å for molecule A and 0.1048 Å for molecule B]. The dihedral angle between the two benzene rings of the salicylaldiminate moiety is only 6.4° for molecule A and of 9.4° for molecule B. The benzene ring of the tosyl group is clearly outside the aforementioned plane with dihedral angles of 58.4° for molecule A and 58.9 ° for molecule B. It is worth noting that the presence of a planar unit in the molecule is important to facilitate intercalation between the DNA bases and thus the cleavage action mechanism. For that reason the study of the planarity of the ligands and their complexes is one of the goals of their description.

**Table S2.** Selected Bond Distances (Å) and angles (°) for H<sub>2</sub>L<sup>1</sup>.

Molecule A		Molecule B	
N(12)-C(19)	1.317(11)	N(22)-C(29)	1.277(12)
N(12)-C(110)	1.434(10)	N(22)-C(210)	1.397(11)
C(11)-O(11)	1.311(10)	C(21)-O(21)	1.295(11)
C(12)-O(12)	1.377(13)	C(22)-O(22)	1.354(13)
C(16)-C(19)-N(12)	120.4(8)	C(26)-C(29)-N(22)	122.2(8)
C(19)-N(12)-C(110)	123.1(8)	C(29)-N(22)-C(210)	123.4(9)

Due to the low quality of the crystallographic data, the positions of the hydrogen atoms of one water molecule have not been determined with the required accuracy. As a consequence, intra and intermolecular interactions in the compound have not been analyzed in detail, although the study of the Hirshfeld surfaces (see below) helps us to understand the intermolecular ones.

### Crystal packing of the compounds **1, 3, 4, 6, 7.**

#### Crystal packing of $[\text{CuL}^1(\text{H}_2\text{O})]\cdot\text{H}_2\text{O}$ (**1**).

This compound was crystallized (see main text) in two different space groups, a triclinic *P*-1 form (**1a**) and an orthorhombic *P<sub>ca</sub>2<sub>1</sub>* analogue (**1b**). Difference between them is at the orientation of the *N*<sup>1</sup>-tosylbenzene unit (Figure S1). In the main text Figure 1 shows an ORTEP sketch of monoclinic **1a**, Figure S6 shows an ORTEP diagram of the orthorhombic **1b**.

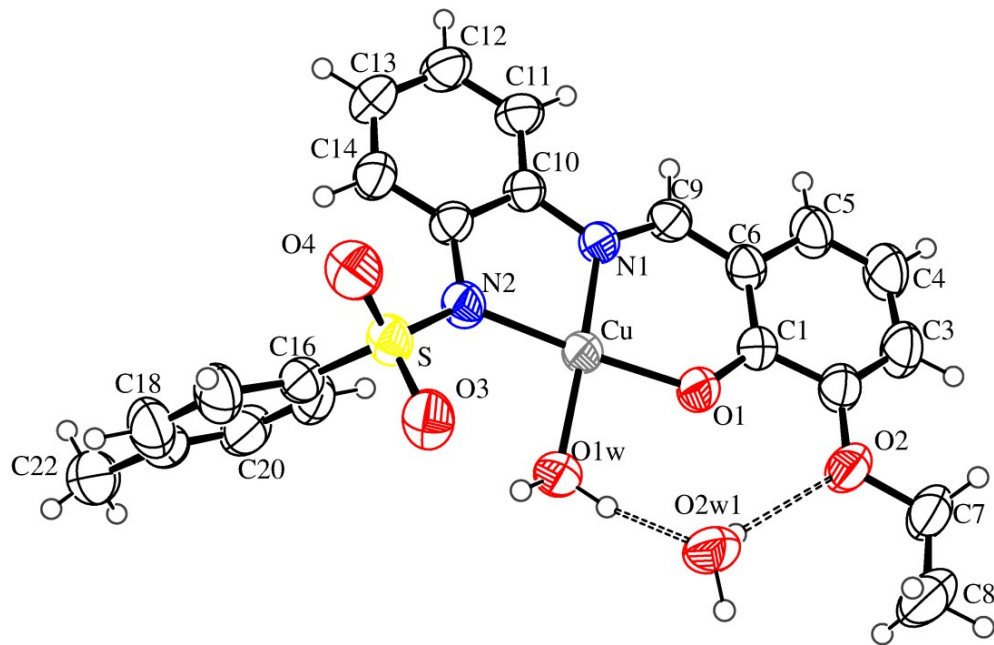


**Fig. S6** ORTEP diagram of the molecular structure of orthorhombic  $[\text{CuL}^1(\text{H}_2\text{O})]\cdot\text{H}_2\text{O}$  (**1b**) showing intra and intermolecular hydrogen bonds.

In both isomers, the  $[\text{CuL}^1(\text{H}_2\text{O})]\cdot\text{H}_2\text{O}$  entity contains two water molecules, one coordinated to the metal atom and another interacting through hydrogen bonds with the

coordinated water molecule and oxygen atom [O(3)] of the tosyl group (Table S3). It should be noted that oxygen atom of the crystallization water is split over two positions with occupancy factor of 0.57(4):0.43(4) for (**1a**) and 0.66(6):0.34(6) for (**1b**). Only one of them is shown in figures. An important difference between **1a** and **1b** is the presence only in **1a** of a weak interaction involving the metal ion and an oxygen atom of the sulfonic group of a neighboring molecule, and also a C-H $\cdots\pi$  interaction. The presence of this weak interaction [distance Cu-O = 2.7566(18) Å] does not affect significantly the Cu-donor bond distances, and thus the complex may be regarded as square planar rather than square-pyramidal. These interactions generate chains of complexes parallel to the crystallographic axis *a*, as seen in Figure S7.

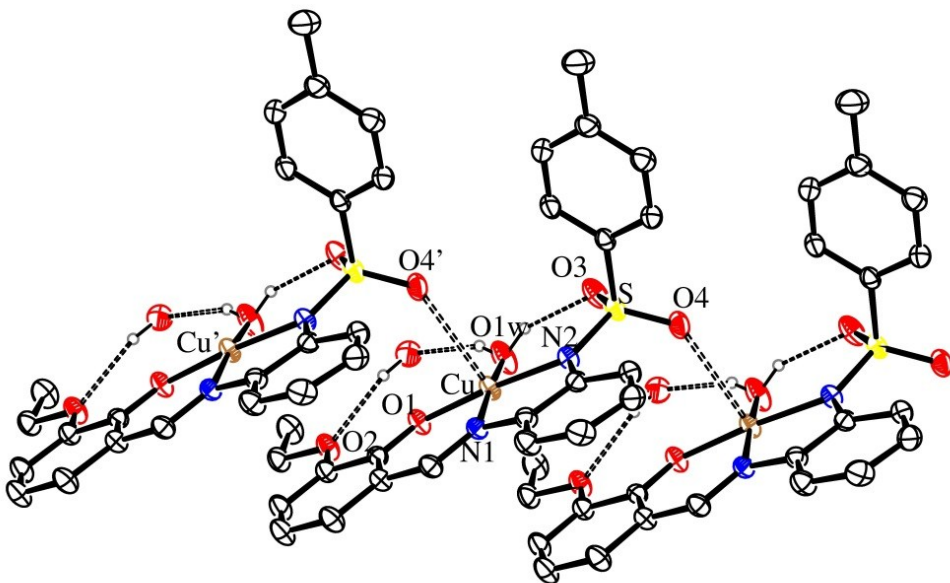


**Fig. S7** The Cu...O interactions in **1a** generate chains of complexes parallel to the crystallographic *a* axis.

In the study of the planarity of the complexes, whatever the isomer, the whole ligand salicylaldiminato [19 atoms, even the ethoxy group, only excluding the sulfone] adopts a nearly planar structure [rms deviation 0.0472 or 0.0259 Å, Cu atom 0.049(1) or 0.138 (2) Å out of the plane]. In fact, the dihedral angle between the two benzene rings are only 2.6(2) and 0.2(2). Note

however that the position of the coordinated water is slightly different in the triclinic and in the orthorhombic isomers. The copper metal are involved in two fused 5-membered CuC<sub>2</sub>N<sub>2</sub> and 6-membered CuC<sub>3</sub>NO metallacycles, and they are mainly planar. In the other hand, the benzene ring of the *p*-toluenyl group is almost perpendicular to the abovementioned plane [dihedral angles of 89.58(6) and 81.9(1) $^{\circ}$ ], and their positions produces the difference between the two isomers. The sulfur atom deviates in (**1a**) 0.254(2) Å over the plane, but in (**1b**), this atom deviates 0.341(4) Å from the plane, as can see in Figure S1. In addition, coordinated water show difference between isomers, since it is in fact coplanar in (**1a**), deviating only 0.153(3) Å but deviates 0.653(5) Å below the plane, in (**1b**).

**Table S3.** Hydrogen bonds and C-H $\cdots\pi$  interactions for **1a** and **1b** [Å and  $^{\circ}$ ].

Donor-H $\cdots$ Aceptor	D-H	H $\cdots$ A	D $\cdots$ A	D-H $\cdots$ A
<b>(1a)</b>				
O(1W)-H(1W1)...O(3)	0.81(5)	1.90(5)	2.593(3)	143(4)
O(1W)-H(1W2)...O(2W1)	0.73(4)	1.92(4)	2.596(7)	154(5)
O(1W)-H(1W2)...O(2W2)	0.73(4)	2.02(4)	2.721(6)	161(5)
O(2W1)-H(2W1)...O(2)	0.83(3)	2.17(3)	2.962(7)	158(3)
O(2W2)-H(2W1)...O(2)	0.89(3)	2.17(3)	3.030(6)	164(3)
C(11)-H(11) $\cdots$ Ct1 <sup>ii</sup>	0.93	2.96	3.753(3)	144
<b>(1b)</b>				
O(1W)-H(1B)...O(1)	0.917(3)	2.460(2)	2.617(4)	89.43(18)
O(1W)-H(1A)...O(3)	0.814(3)	2.001(3)	2.608(5)	131.0(2)
O(1W)-H(1B)...O(2W1)	0.917(3)	1.763(15)	2.668(13)	168.6(8)
O(1W)-H(1B)...O(2W2)	0.917(3)	1.75(3)	2.62(2)	159(2)
O(2W1)-H(2A)...O(3 <sup>i</sup> )	0.90(5)	2.02(5)	2.898(10)	165(5)
O(2W2)-H(2A)...O(3 <sup>i</sup> )	1.04(6)	2.02(5)	2.89(2)	140(5)

Symmetry transformations used, i: 1-x, 1-y, z-1/2; ii: x, y-1, z;  $\gamma$  is the angle between Cg-H vector and ring normal.

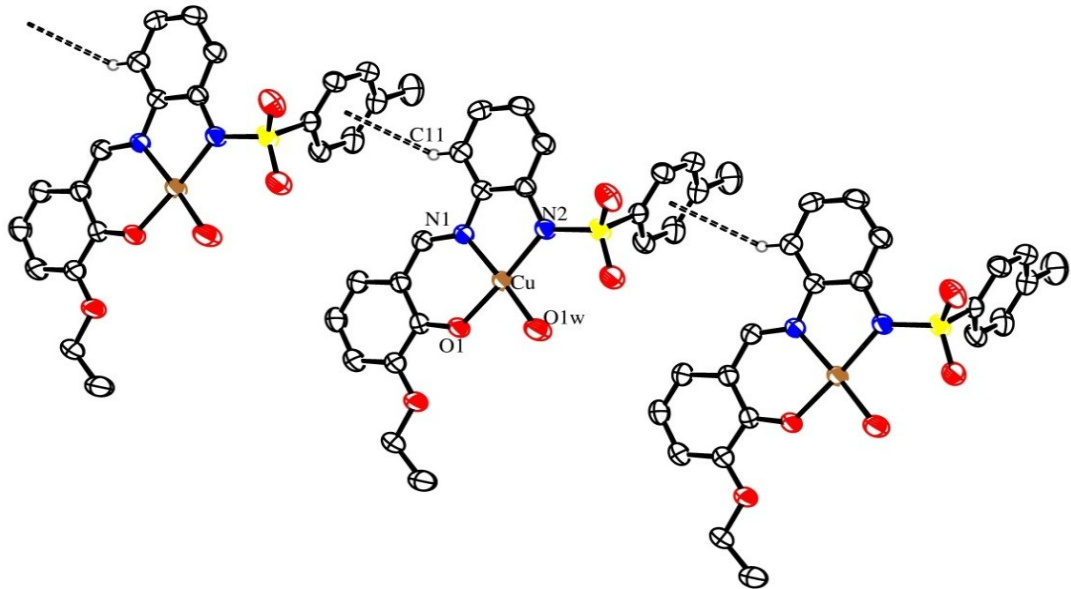


**Fig. S8** Growing along *b* axis for **1a**, see parameters in **Table S3** above.

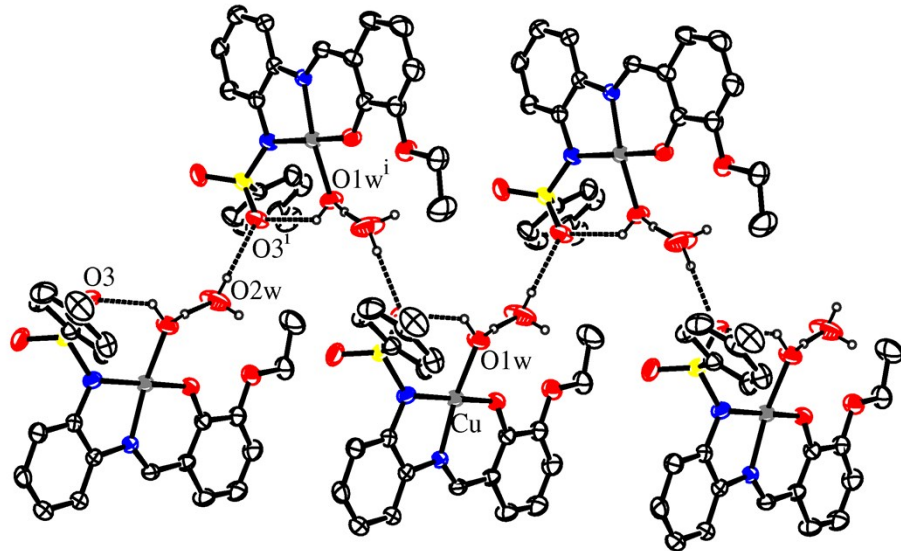


**Fig. S9** Crystal packing diagram for **1b** showing the interactions H...OH.

In both isomer, classical interactions OH...O (Table S3) occur within the same asymmetric unit, both intra and intermolecular (Figures S6 and S7). The intramolecular interaction takes place between the oxygen of the metal coordinated water O(1W) and oxygen atom O(3) of the tosyl group nearest to it, while the intermolecular takes place between oxygen

O(1W) and oxygen atom from molecule of water of crystallization O(2W). Only in the case of **1a** a C-H $\cdots\pi$  interaction is also found between the diaminebenzene ring and the toluene one, as is shown in Figure S8. Such interactions do not exist in **1b**, due to the zig-zag packing of the molecules in the crystal (Figure S9).

### Crystal packing of $[\text{Cu}_2\text{L}^1_2(4,4'\text{-bpy})_3]$ (**3**).

A brief description of this compound can be found in the main text. Other features worthy to note are the planarity of the whole complex **3**, (Figure S10) in such a way that the benzene ring of the tosyl groups is situated almost parallel to the 16 membered Schiff base [dihedral angle of 25.0(2) $^\circ$ ] and allows a  $\pi,\pi$ -stacking interaction with the 4,4'-bpy ligand of a neighboring molecule (1-x, 1-y, 2-z) as can be seen in Figure S11 and parameters in Table S4, giving a crystal growing in zig-zag along the  $a$  axis. Also in the crystal packing, some C-H $\cdots\text{O}$  interaction between neighboring molecules can be found, and they produce a growing of the crystal along the zone axis ( $\bar{1}, 1, 0$ ), as is shown in Figure S12, with the parameters indicated in Table S5.

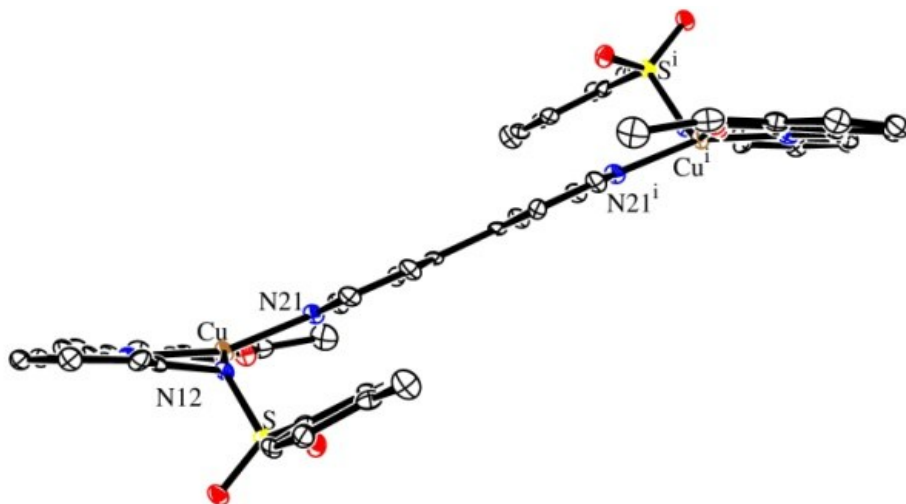


**Fig. S10** View of the molecule **3** through the 4,4'-bpy plane.

**Table S4.** Parameters of the  $\pi,\pi$ -stacking interactions for  $[\text{Cu}_2\text{L}^1_2(4,4'\text{-bpy})]$  (**3**).

Interaction	$\text{Cg}\cdots\text{Cg}^a$	$\alpha$	$\beta$	$\gamma$
$\text{Cg1-Cg2}^i$	3.593(2)	4.00(19)	22.37	18.87

<sup>a</sup>Cg1 is the centroid of the bipyrimidine ligand, Cg2 is the centroid of the tosyl benzene. Symmetry operation, i: 1-x, 1-y, 2-z

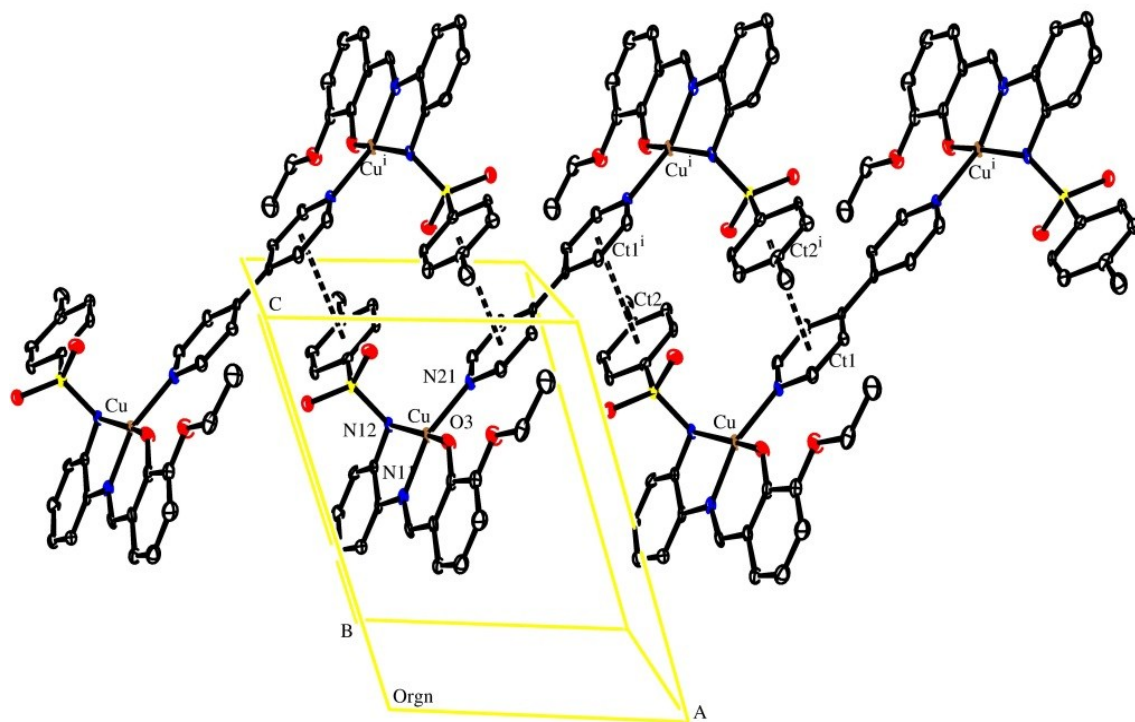


**Fig. S11** Crystal packing diagram of **3** showing  $\pi,\pi$ -stacking interactions.

**Table S5.** Hydrogen bond parameters for  $[\text{Cu}_2\text{L}^1_2(4,4'\text{-bpy})]$  (**3**) [ $\text{\AA}$  and  $^\circ$ ].

D-H...A	d(D-H)	d(H...A)	d(D...A)	$\angle(\text{DHA})$
C(19)-H(19)...O(1 <sup>i</sup> )	0.95	2.56	3.486(5)	164.3
C(111)-H(111)...O(1 <sup>i</sup> )	0.95	2.47	3.394(5)	163.9
C(21)-H(21)...O(3)	0.95	2.23	2.789(5)	116.8
C(25)-H(25)...N(12)	0.95	2.58	3.162(5)	119.5
C(117)-H(117)...O(1)	0.95	2.55	2.912(5)	102.5

Symmetry operation, i: -x, -y, 1-z.

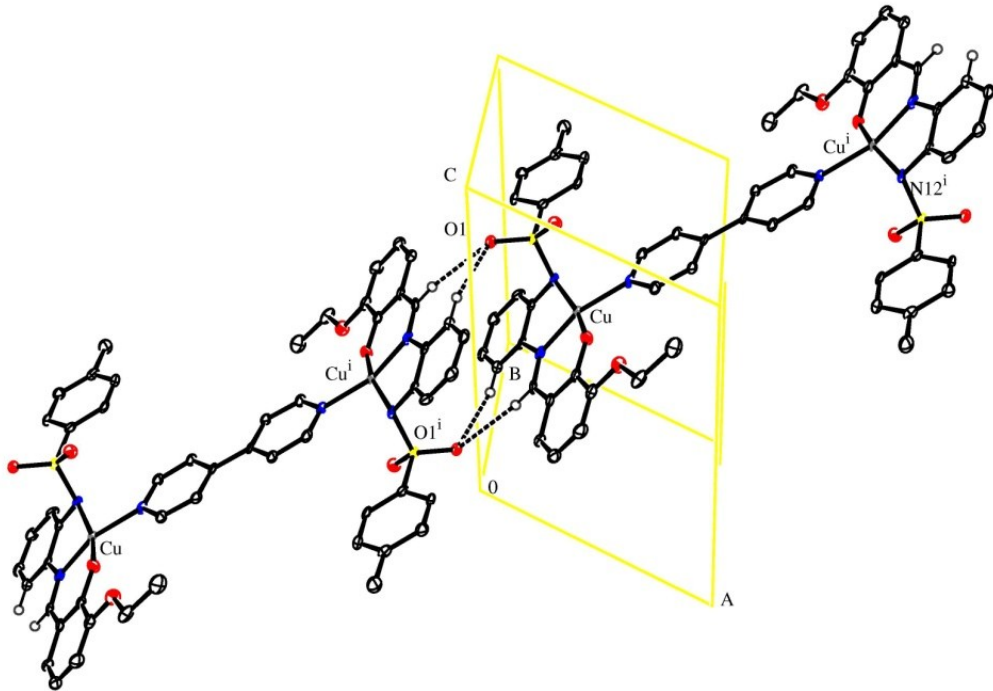


**Fig. S12** Crystal packing diagram of **3** showing some as C-H···O interactions.

#### Crystal packing of [CuL<sup>1</sup>(phen)] (**4**).

A brief description of these compounds can be found in the main text, including the ORTEP drawn of the crystal structure. Crystal packing in **4** is the result of the presence of both intra and intermolecular interactions and even some non-conventional CH···O hydrogen bond. Among later ones, the most interesting are between the C(112) of a fragment diaminobenzene group and oxygen O(12) of the tosyl group and between the carbon C(115) of the tosyl group and the other oxygen O(1) of the same tosyl group (Table S6). Among the intermolecular interactions to generate a 3D network there are strong intermolecular  $\pi$ - $\pi$  interactions (Table S7 and Figure S2), which takes place between a pyridine ring of a molecule of 1,10-phenanthroline and the benzene ring of other 1,10-phenanthroline neighbouring molecule complex [ $Ct(1)\text{-}Ct(2^i) = 3.4820(2)$  Å], producing dimeric units. There are also CH···O interactions, established between the carbon atoms C(116) and C(23), belonging to a tosyl group or to a phenanthroline molecule, and the

oxygen O(11) and O(12) belonging to tosyl groups of a contiguous asymmetric unit (Table S6). These CH $\cdots$ O links result in a chain of complexes along the crystallographic *b* axis, shown in Fig. S13. Additionally, this compound crystallized together with an acetonitrile solvent molecule, but it was not modelled due its disorder.

**Table S6.** Parameters of the hydrogen bonds in [CuL<sup>1</sup>(phen)] (**4**).

Donor-H $\cdots$ Aceptor	d(D-H)	d(H $\cdots$ A)	d(D $\cdots$ A)	<D-H $\cdots$ A (°)
C(112)-H(112)...O(12)	0.93	2.31	2.880(4)	119.5
C(115)-H(115)...O(11)	0.93	2.51	2.885(4)	104.6
C(116)-H(116)...O(11i)	0.93	2.48	3.404(4)	171.8
C(23)-H(23)...O(12i)	0.93	2.51	3.334(4)	148.2

Symmetry transformation used to generate equivalent atoms: i= 0.5-x, y-0.5, 0.5-z

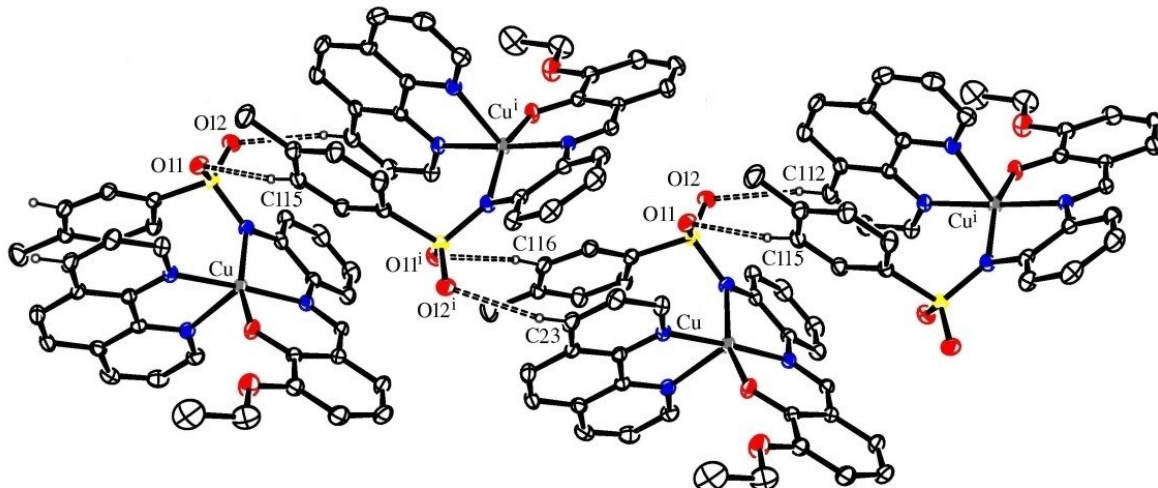


**Fig. S13** Intermolecular C-H $\cdots$ O interactions in **4**.

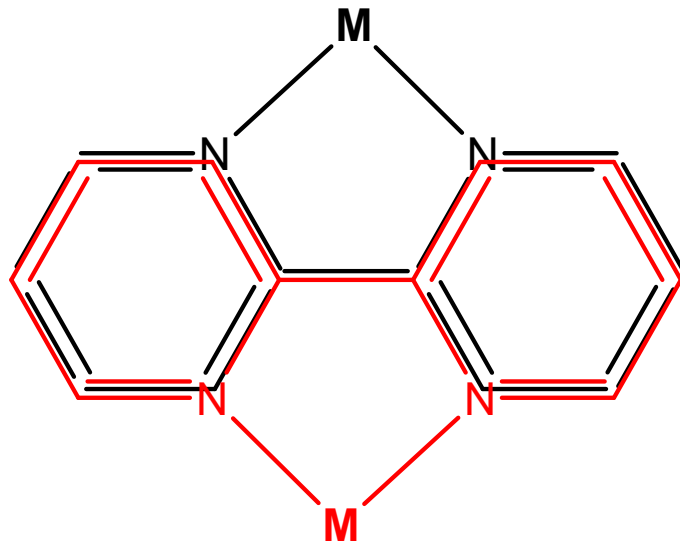
**Table S7.** Parameters of the  $\pi,\pi$ -stacking interactions in [CuL<sup>1</sup>(phen)] (**4**).

Interacción	Cg $\cdots$ Cg [Å]	$\alpha$	$\beta$	$\gamma$
Cg(1)-Cg(2)	3.525(3)	6.1(2)	15.5	17.0
Cg(3)-Cg(2i)	3.482(2)	0.7(2)	11.1	11.6

Symmetry operation: i = 0.5-x, 1.5-y, -z.

### Crystal packing of $[\text{CuL}^2(2,2'\text{-bpy})]$ (6).

In the case of compound  $[\text{CuL}^2(2,2'\text{-bpy})]$  (6), there are several no-conventional C-H $\cdots$ X (X = O, N) intermolecular hydrogen bonds and two  $\pi,\pi$ -stacking interactions in the crystal packing. Two of the hydrogen bonds (Table S8) take place between C(28)-H and C(27)-H belonging to a 2,2'-bipyridine ligand, and the oxygen O(12) of the tosyl group and amide nitrogen N(11), respectively, both from the adjacent asymmetric unit. These are reinforcing a strong  $\pi\cdots\pi$  interaction (Table S9), of type 'face to face', that takes place between the centroids of the rings containing the oxygen atom of the naphthalate group from two neighboring asymmetric units. Another  $\pi\cdots\pi$  interaction takes place between the rings of 2,2'-bipyridine complex of neighboring units (Scheme S1). The four above mentioned intermolecular interactions lead to chain of complexes along crystallographic *b* axis, as shown in Figure S14.



**Scheme S1** Overlap along the *b* axis of the 2,2'-bipyridine rings of two neighboring molecules of 6.

**Table S8.** Hydrogen bonds for  $[\text{CuL}^2(2,2'\text{-bpy})] (\mathbf{6})$ . [Å and °].

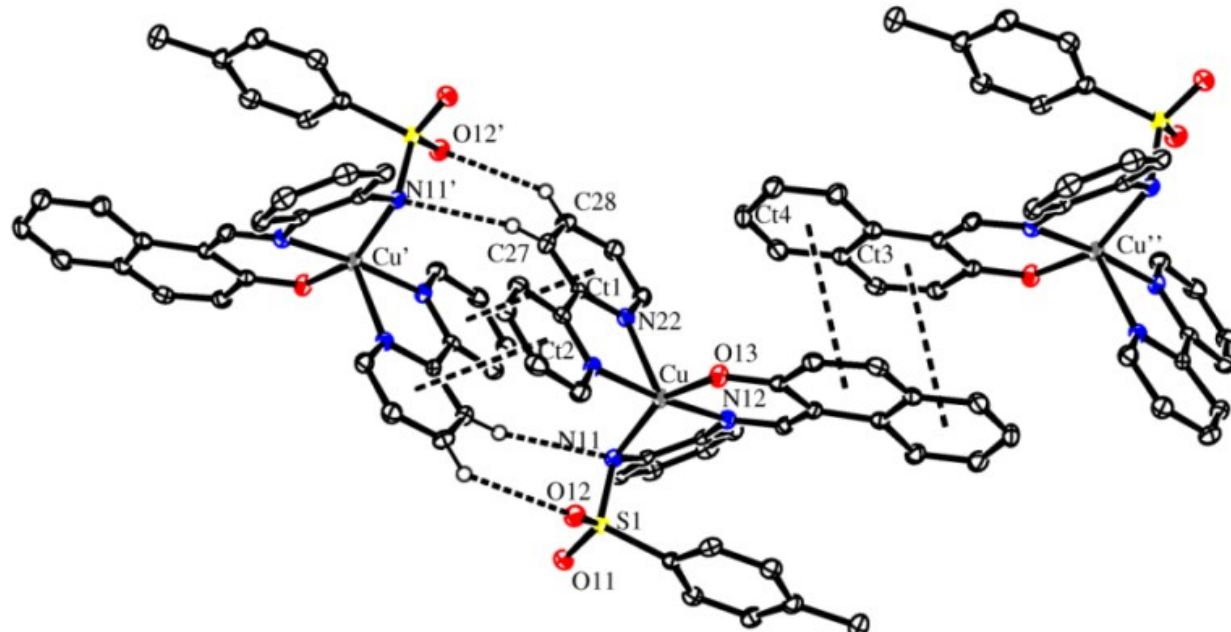
Donor-H $\cdots$ Aceptor	d(D-H)	d(H $\cdots$ A)	d(D $\cdots$ A)	$\angle\text{D-H}\cdots\text{A}$ (°)
C(27)-H(27)...N(11 <sup>i</sup> )	0.95	2.59	3.451(3)	151.7
	0.95	2.55	3.268(3)	132.8
C(28)-H(28)...O(12 <sup>i</sup> )				
C(23)-H(23)...O(11 <sup>iii</sup> )	0.95	2.66	3.147(3)	112.2
C(122)-H(122)...O(12 <sup>iv</sup> )	0.95	2.71	3.447(3)	135.0

Symmetry transformations used to generate equivalent atoms: i: 2-x, 2-y, -z; iii: 1+x, y, z; iv: 2-x, y-1/2, 1/2-z.

**Table S9.** Parameters of the  $\pi$ -stacking interactions for  $[\text{CuL}^2(2,2'\text{-bpy})] (\mathbf{6})$ .

Interaction	Cg $\cdots$ Cg [Å]	$\alpha$	$\beta$	$\gamma$
Cg1-Cg2 <sup>i</sup>	3.7134(15)	8.69	22.50	17.48
Cg3-Cg4 <sup>ii</sup>	3.6602(15)	0.00	16.11	16.11

Cg1 and Cg2 are the centroids of the bipyridine ligand; Cg3 and Cg4 are the centroids of the naphthalate group; symmetry operations: i: 2-x, 2-y, -z; ii: 2-x, 1-y, -z.

**Fig. S14** ORTEP view of **6** showing the  $\pi,\pi$ -stacking and some C-H $\cdots$ X (X = N, O) interactions.

### Crystal packing of $[\text{Cu}_2\text{L}^2(4,4'\text{-bpy})_3]$ (7)

As is mentioned in the main text,  $[\text{Cu}_2\text{L}^2(4,4'\text{-bpy})_3]$  (7) is composed of dinuclear units where one half is symmetry generated ( $1-x$ ,  $1-y$ ,  $-z$ ). There are one and a half crystallographically different 4,4'-bipyridine coordination ligands in the asymmetric unit. One of the 4,4'-bipyridine ligands behaves as a monotopic ligand. One of the nitrogen atoms in the pyridine ring, labelled as N(31), is coordinated to the copper atom and the other one, labelled as N(32), is implicated in the supramolecular network, since forms a  $\text{CH}\cdots\text{N}$  interaction with a methyl group of a neighbouring molecule ( $\text{C}\cdots\text{N}$  distance of  $3.360(3)$  Å). The other 4,4'-bpy ligand contains an inversion center at the middle of the C-C bond that relates the two half molecules. This 4,4'-bpy molecule behaves as a ditopic ligand that connects the two copper ions.

The Schiff base ligand in this compound is not planar, with a dihedral angle involving the naphthalene ring and the benzene ring of  $44.52(8)^\circ$ . This behavior contrasts with that of compound **3**, where the Schiff base fragment is essentially planar. This angle is bigger to that found in the compound **3**, but now, no intermolecular  $\pi\cdots\pi$  stacking interactions were found, although an  $\text{C-H}\cdots\text{N}$  bond is present, between one carbon atom in the tolyl ring, C(122), and the nitrogen atom of the neighbor 4,4'-bipyridine, the unique nitrogen atom in the molecule not bonded to the metal, so free to form such interactions.

**Table S10.** Parameters of the  $\pi,\pi$ -stacking interactions for (7).

Interaction	$\text{Cg}\cdots\text{Cg}^a$	$\alpha$	$\beta$	$\gamma$
$\text{Cg1-Cg1}^{iv}$	$3.8614(9)$	$0.00$	$21.51$	$21.51$

<sup>a</sup>Cg1 is the centroid of the bipyridine ligand. Symmetry operation; iv:  $3-x, -y, -z$ .

The supramolecular network is building both with  $\pi,\pi$ -stacking interactions established between the free pyridine rings of the terminal 4,4'-bipyridine ligand of vicinity dimeric molecules (parameters are set out in Table S10) and a CH $\cdots$ N interaction between same molecules (see Table 11), causing a growing in the along the zone axis (1,1,0), as is shown in Figure S15. Additionally there are several CH $\cdots$ O and C $\cdots$ H- $\pi$  interactions (see Table S11), that cause the growing in other space directions, resulting a 3D grid. The benzene ring of the tosyl groups is situated almost parallel to the 16 membered Schiff base [dihedral angle of 25.0(2) $^{\circ}$ ] and allows a  $\pi,\pi$ -staking interaction with the 4,4'-bpy ligand of a neighboring molecule (1-x, 1-y, 2-z), as can be seen in Figure S15 and parameters in Table S11 giving a crystal growing in zig-zag along the  $a$  axis. The crystal packing is also conditioned by some C-H $\cdots$ O interactions between neighbouring molecules, they are show in Figure S16, and they produces a growing in the  $a$  axis.

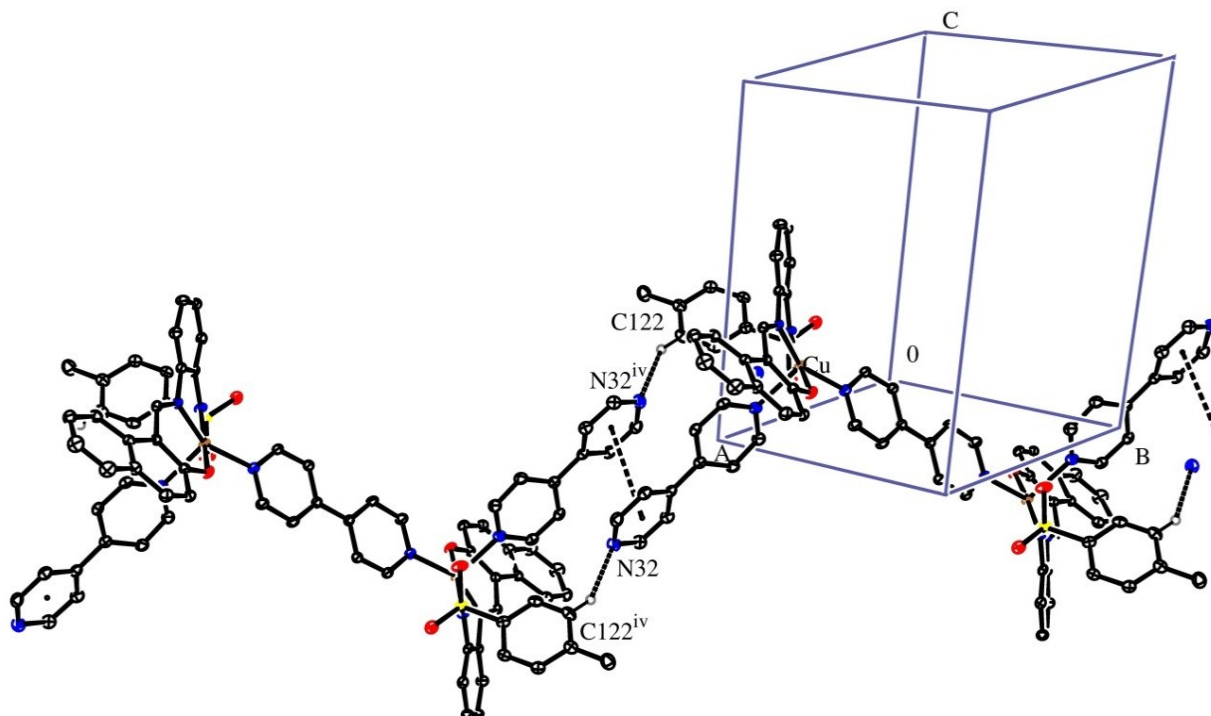


**Fig. S15** Crystal packing diagram of 7 showing  $\pi,\pi$  -stacking interactions and a C-H $\cdots$ N interaction.

**Table S11.** Hydrogen bonds parameters for  $[\text{Cu}_2\text{L}^2(4,4'\text{-bpy})_3]$  (**7**) [ $\text{\AA}$  and  $^\circ$ ].

D-H...A	d(D-H)	d(H...A)	d(D...A)	$\angle(\text{DHA})$
C(31)-H(31)...O(1)	0.93	2.70	3.115(3)	107.7
C(34)-H(34)...O(2 <sup>ii</sup> )	0.93	2.53	3.378(3)	151.7
C(39)-H(39)...O(1 <sup>ii</sup> )	0.93	2.39	3.148(3)	138.8
C(115)-H(115)...O(2 <sup>iii</sup> )	0.93	2.51	3.334(3)	148.4
C(122)-H(122)...N(32 <sup>iv</sup> )	0.93	2.59	3.360(3)	140.3
C(113)-H(113)...Ct2 <sup>v</sup>	0.93	2.73	3.584(2)	152.6
C(13)-H(13)...Ct1 <sup>vi</sup>	0.93	2.66	3.563(2)	163.8
C(124)-H(12C)...O(11 <sup>vii</sup> )	0.96	2.75	3.625(3)	152.1

Symmetry operations; ii:  $x+1, y, z$ ; iii:  $1-x, -y, 1-z$ ; iv:  $3-x, -y, -z$ ; v:  $2-x, -y, 1-z$ ; vi:  $3-x, 1-y, -z$ ; vii:  $x, y-1, z$ .

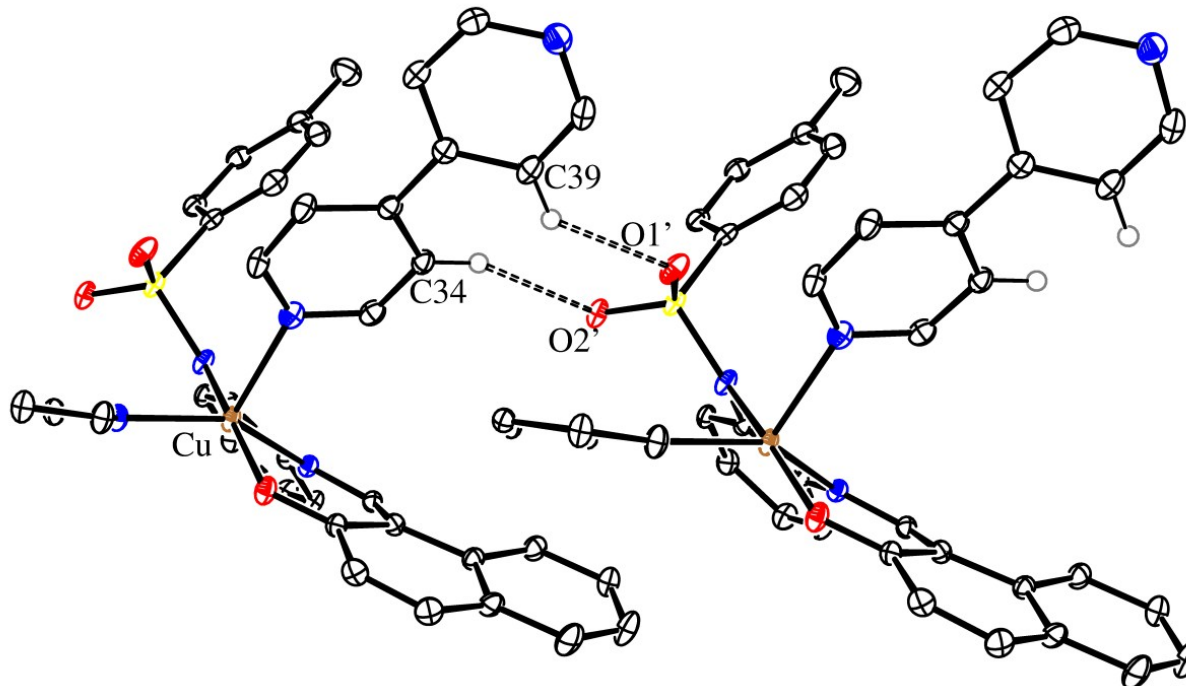


**Fig. S16** C-H···O interactions in **7**. Only two half of molecules were drawn in the sake of clarity.

### Hirshfeld surface analysis.

The Hirshfeld surfaces were calculated using the Crystal Explorer v.3.1 program package and the 2D fingerprint was prepared using the same software.<sup>6</sup> This technique allows the vision of the interactions in crystal structures.<sup>7</sup> The method uses visual recognition of several properties of intermolecular interactions through mapping onto this surface (curvedness, shape index,  $d_{\text{norm}}$ , etc.). Surfaces were drawn in this paper by the representation of the *normalized contact distance*,  $d_{\text{norm}}$ , defined as the sum of the normalised by the van der Waals radius of the atom involved  $d_i$  and  $d_e$ .<sup>8</sup> The  $d_i$  and  $d_e$  are defined, respectively, as the distance from the Hirshfeld surface to the nearest nucleus outwards from the surface and the distance from the surface to the nearest atom in the molecule itself. The use of surface curvature is also an interesting tool for the study of the interactions of the molecules,<sup>9a=7a</sup> so surfaces mapped with *curvedness* and *shape index* are provided for each crystal structure studied in this paper. Finally, all ( $d_i$ ,  $d_e$ ) contacts can be expressed in the form of a two dimensional plot, known as the 2D fingerprint plot.<sup>9</sup> The shape of this plot, which is unique for each molecule, is determined by dominating intermolecular contacts. The 2D fingerprint plot were constructed by using reciprocal interactions, that is, both X...Y and Y...X interactions were included in the fingerprints. The input of the program is always the deposited cif file, but in the case of **4**, a "made-up" cif file was generated where the atom positions of the solvent MeCN are included, even the hydrogen atoms on the methyl group.

*Hirshfeld surface analysis of H<sub>2</sub>L<sup>1</sup>·H<sub>2</sub>O.* The two independent molecules found in the asymmetric unit of H<sub>2</sub>L<sup>1</sup>·H<sub>2</sub>O were considered and studied as independent ones. Figure S17 shows the front and back Hirshfeld surface modeled on  $d_{\text{norm}}$  (rotated by 180° around the vertical axis of the plot) for one of these molecules of H<sub>2</sub>L<sup>1</sup>·H<sub>2</sub>O, shown as transparent to allow the visualization of the molecules, and evidence the red spots. Note that the most important

interactions are those with the position of the water molecule, but, as was stated in the crystallographical section the disorder found for this molecule was not modeled in the cif file, so data obtained here could be taken with caution. Figure S18 shows again the front and back surfaces for the other molecule in the asymmetric unit of  $\text{H}_2\text{L}^1 \cdot \text{H}_2\text{O}$ . It is worth noting that both surfaces are similar but not identical. Surfaces mapped with curvedness and shape index are also provided in Figures S19 and S20, respectively for one of the molecules of  $\text{H}_2\text{L}^1 \cdot \text{H}_2\text{O}$ . Note that in these figures, only for the molecule labeled as 1x was generated, but the other one was sketched in order to show their interactions.

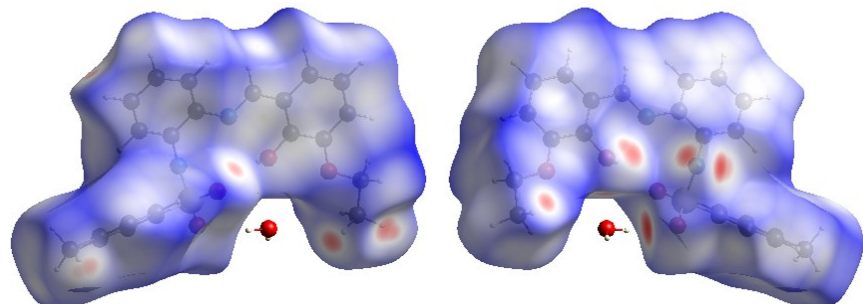


**Fig. S17** View of  $d_{\text{norm}}$  Hirschfeld surface analysis for one of the molecules found in the asymmetric unit of  $\text{H}_2\text{L}^1 \cdot \text{H}_2\text{O}$ . (see text, molecule labeled as 1x).

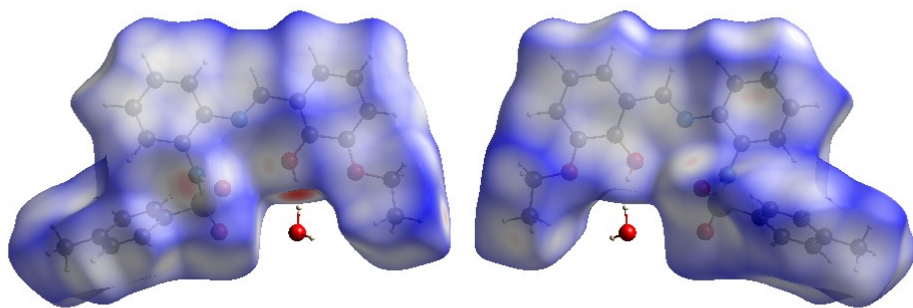


**Fig. S18** View of  $d_{\text{norm}}$  Hirschfeld surface analysis for one of the molecules found in the asymmetric unit of  $\text{H}_2\text{L}^1 \cdot \text{H}_2\text{O}$ . This is for the molecule labeled as 2x.

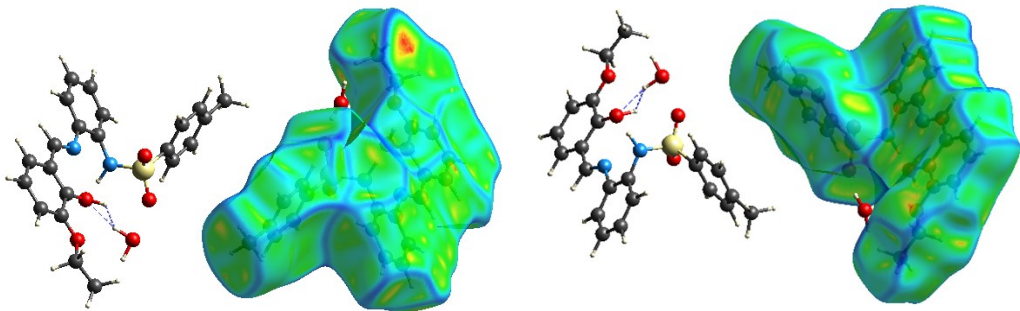


**Fig. S19** View of curvedness surface for one of the molecules found in the asymmetric unit of  $\text{H}_2\text{L}^1 \cdot \text{H}_2\text{O}$ .

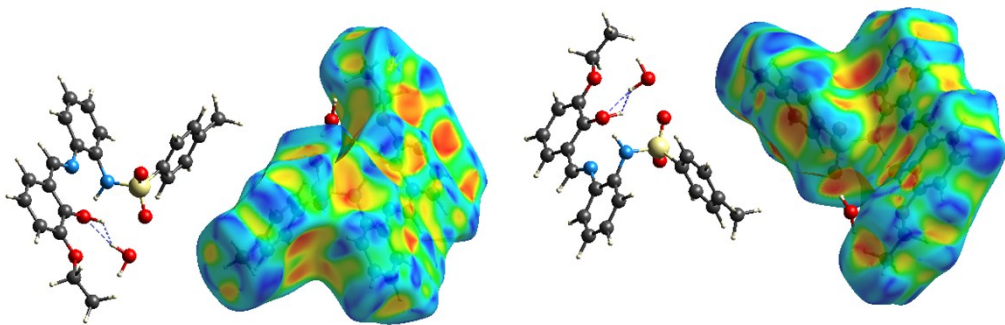


**Fig. S20** View of *shape index* surface for the molecule labeled as 1x of  $\text{H}_2\text{L}^1 \cdot \text{H}_2\text{O}$ .

The above-mentioned 2D fingerprint plots were also studied separately, since, as can be observed in them, the surroundings of both molecules are slightly different. Figure S21 shows them, plotted with the percentage of each contribution. As can be seen, van der Waals forces ( $\text{H}\cdots\text{H}$  contacts, 54.0 and 51.2 %) constitute the majority of forces contributing to the supramolecular network. These figures highlight the differences between two molecules in the asymmetric unit.

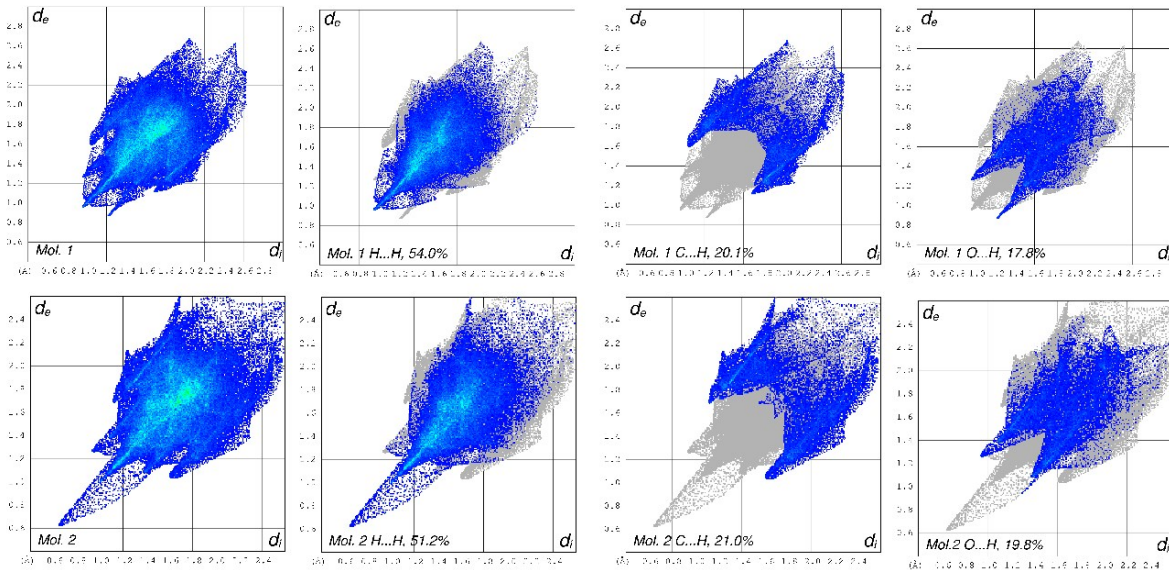


**Fig. S21** 2D fingerprint for  $\text{H}_2\text{L}^1 \cdot \text{H}_2\text{O}$ .

*Hirshfeld surface analysis of  $[\text{CuL}^1(\text{H}_2\text{O})]\text{H}_2\text{O}$*  (**1a**) and (**1b**). Figures S22 and S23 show the front and back surfaces modelled on  $d_{\text{norm}}$  for both polymorphs. As usual, red spots indicate the interactions with the surrounding, and those with the water molecule are the most intense. In these figures some differences could be found between polymorphs. Surfaces mapped with curvedness and shape index are also provided in Figures S24 to S27. On the other hand, Figures S28 and S29 show the 2D fingerprint obtained for these polymorphs,. As expected, they show important difference between them. Percentages of the contributions are given in the fingerprint, and ratify the mentioned in the x-ray descriptions section, with the contribution of  $\text{C-H}\cdots\pi$  interactions more important in the triclinic polymorph than in the orthorhombic one (22.6% vs. 17.3% contribution of the  $\text{C}\cdots\text{H}$  interactions).

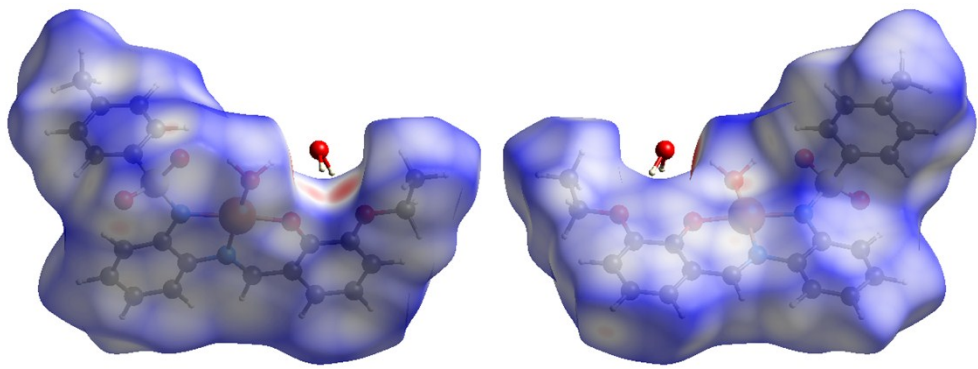


**Fig. S22** View of  $d_{\text{norm}}$  Hirschfeld surface analysis for  $[\text{CuL}^1(\text{H}_2\text{O})]\cdot\text{H}_2\text{O}$  (**1a**).

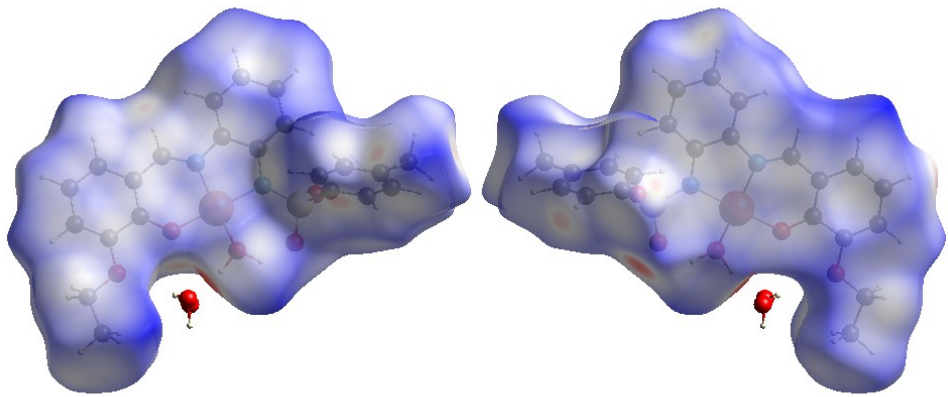


**Fig. S23** View of  $d_{\text{norm}}$  Hirschfeld surface analysis for  $[\text{CuL}^1(\text{H}_2\text{O})]\cdot\text{H}_2\text{O}$  (**1b**).

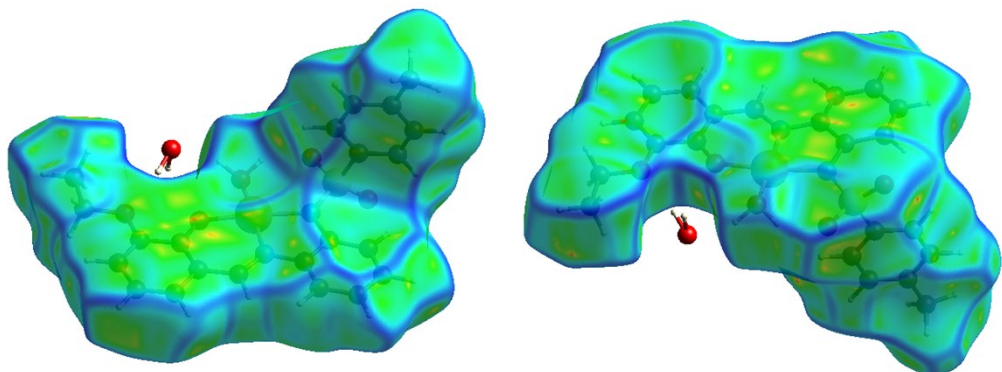


**Fig. S24** View of curvedness surface for  $[\text{CuL}^1(\text{H}_2\text{O})]\cdot\text{H}_2\text{O}$  (**1a**).

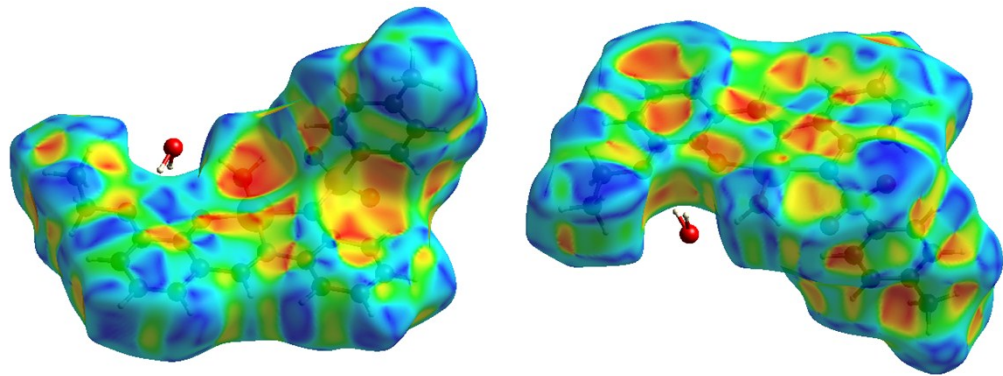


**Fig. S25** View of *shape index* surface for  $[\text{CuL}^1(\text{H}_2\text{O})]\cdot\text{H}_2\text{O}$  (**1a**).

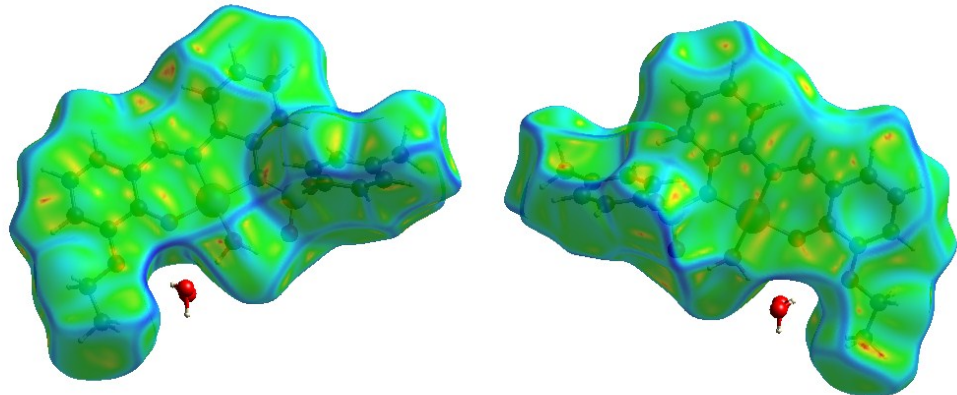


**Fig. S26** View of curvedness surface for  $[\text{CuL}^1(\text{H}_2\text{O})]\cdot\text{H}_2\text{O}$  (**1b**).

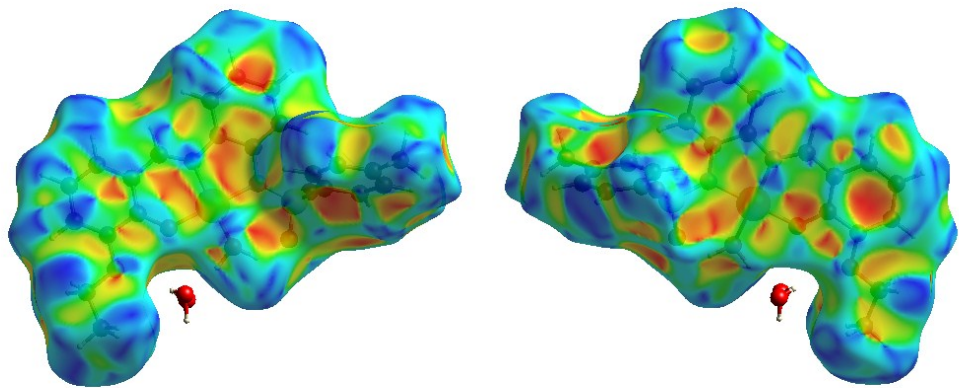


**Fig. S27** View of *shape index* surface for  $[\text{CuL}^2(\text{H}_2\text{O})]\cdot\text{H}_2\text{O}$  (**1b**).

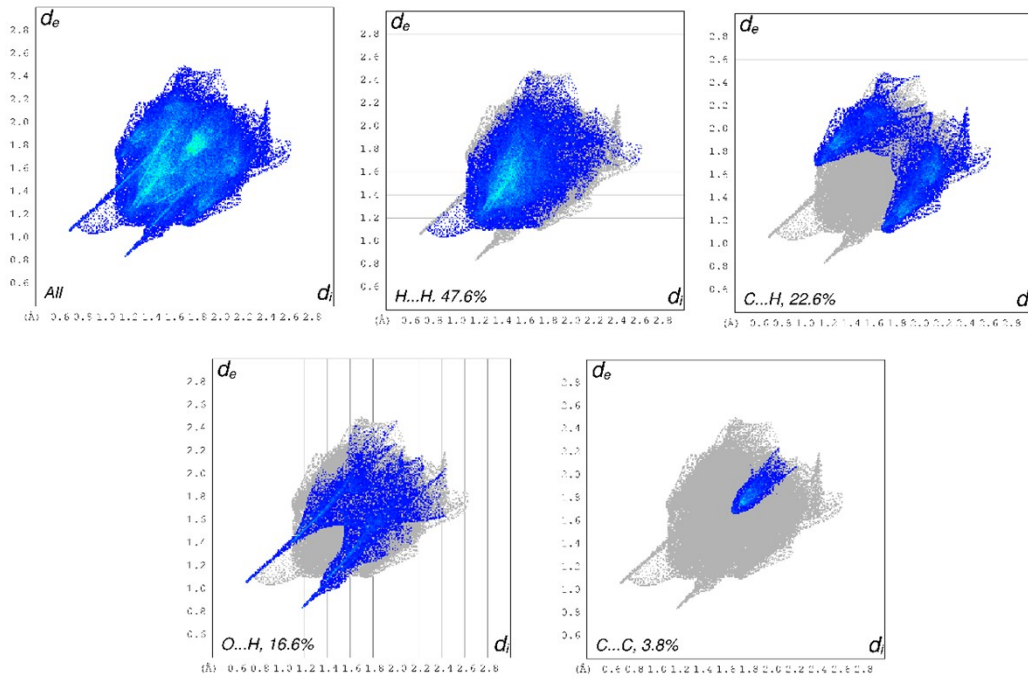


**Fig. S28** 2D fingerprint for  $[\text{CuL}^1(\text{H}_2\text{O})]\cdot\text{H}_2\text{O}$ , triclinic (**1a**).

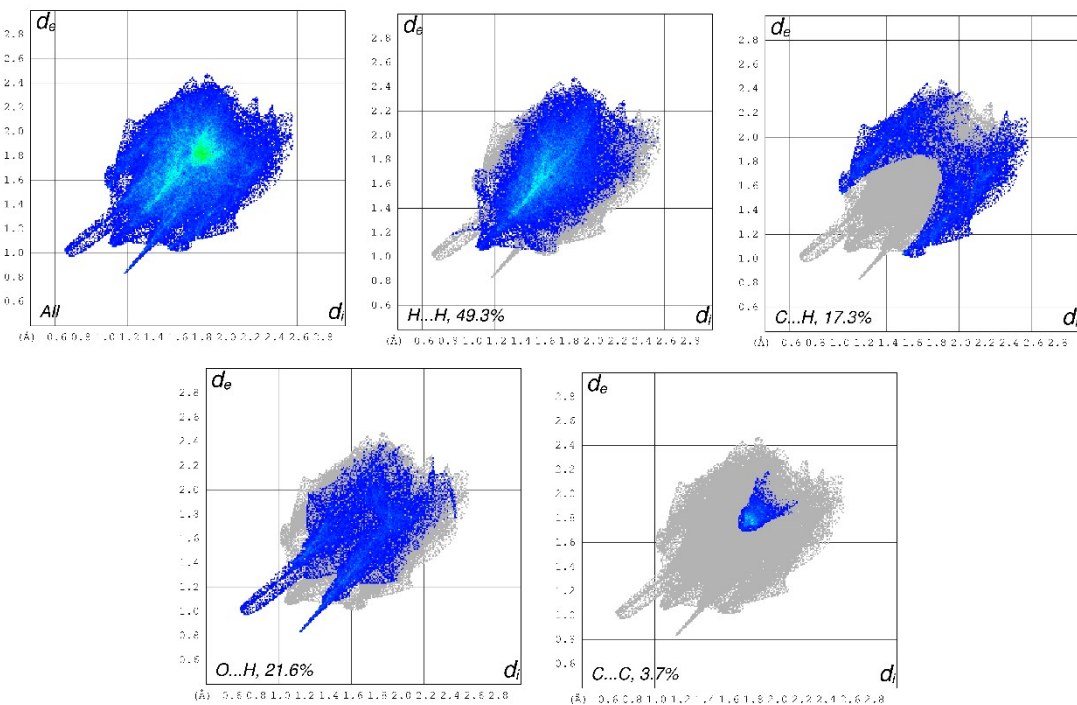


**Fig. S29** 2D fingerprint for for  $[\text{CuL}^1(\text{H}_2\text{O})]\cdot\text{H}_2\text{O}$  orthorhombic (**1b**).

*Hirshfeld surface analysis of  $[Cu_2L^1_2(4,4'-bpy)]$  (3).* Figure S30 shows the front and back surfaces modelled on  $d_{norm}$  for  $[Cu_2L^1_2(4,4'-bpy)]$  (3). As we did with compound 7, (see below) the whole dimer of formula  $[Cu_2L^1_2(4,4'-bpy)]$  was studied (note that the asymmetric unit contains a half of it). As usual, red spots indicate the interactions with the surrounding, and it is worth noting those due the C-H...O interactions with the  $SO_2$  group mentioned in the description of the structure. Surfaces mapped with curvedness and shape index are drawn in Figures S31 and S32. Figure S33 shows the 2D fingerprint obtained for this compound, highlighting the individual contribution of each interaction.

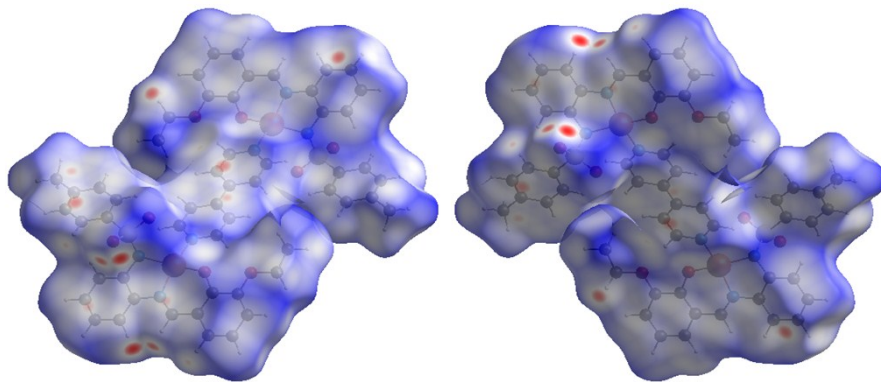


**Fig. S30** View of  $d_{norm}$  Hirshfeld surface analysis for  $[Cu_2L^1_2(4,4'-bpy)]$  (3).

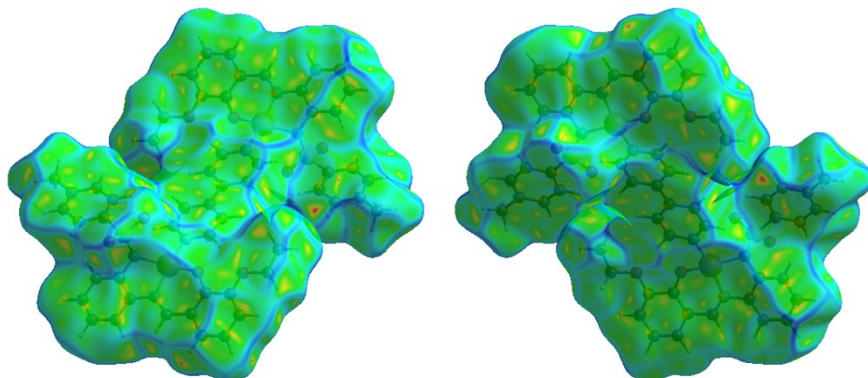


**Fig. S31** View of curvedness surface for  $[Cu_2L^2_2(4,4'-bpy)]$  (3).

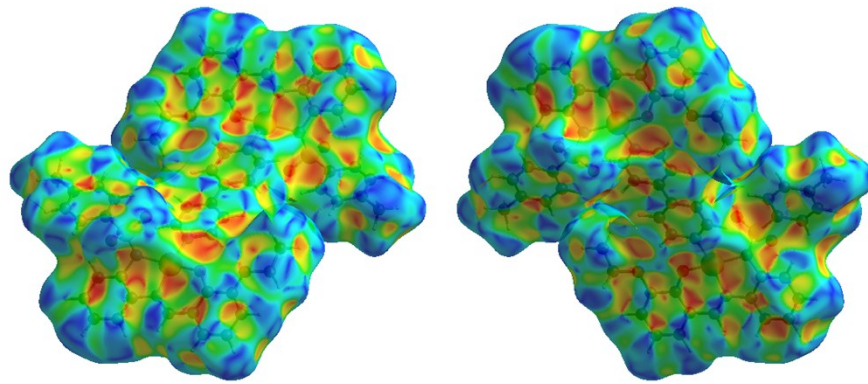


**Fig. S32** View of *shape index* surface for  $[\text{Cu}_2\text{L}^2(4,4'\text{-bpy})]$  (3).

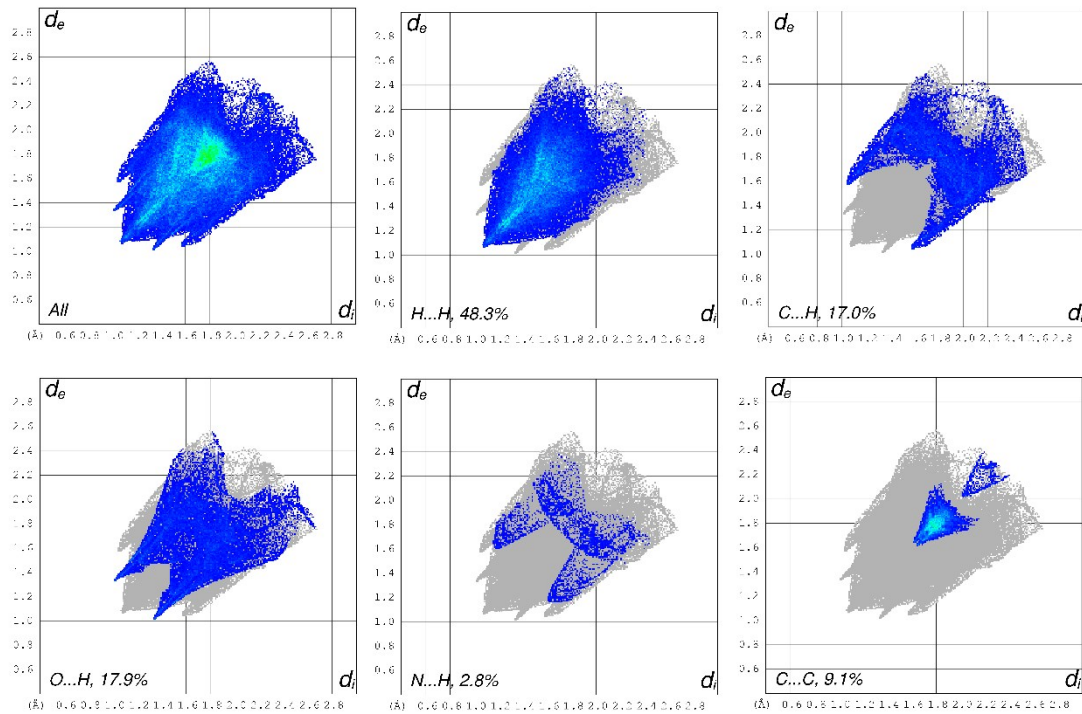


**Fig. S33** 2D fingerprint for  $[\text{Cu}_2\text{L}^2(4,4'\text{-bpy})]$  (3).

*Hirshfeld surface analysis of  $[\text{CuL}^1(\text{phen})]$  (4).* In the case of  $[\text{CuL}^1(\text{phen})]$  (4), and as was stated in the experimental part, there is a molecule of solvent in the crystal, probably MeCN, but the quality of the data does not allow to model this molecule. However, it is very possible that this solvent molecule would be implicated in the macromolecular structure, and for this reason, a

cif file was generated including those atoms. Indeed, in Figure S34 a red spot near the position of the solvent clearly indicates that there is any kind of interaction, unfortunately not studied in the above description of the structure. Surfaces mapped with curvedness and shape index for  $[\text{CuL}^1(\text{phen})]$  (**4**) are drawn in Figures S35 and S36.

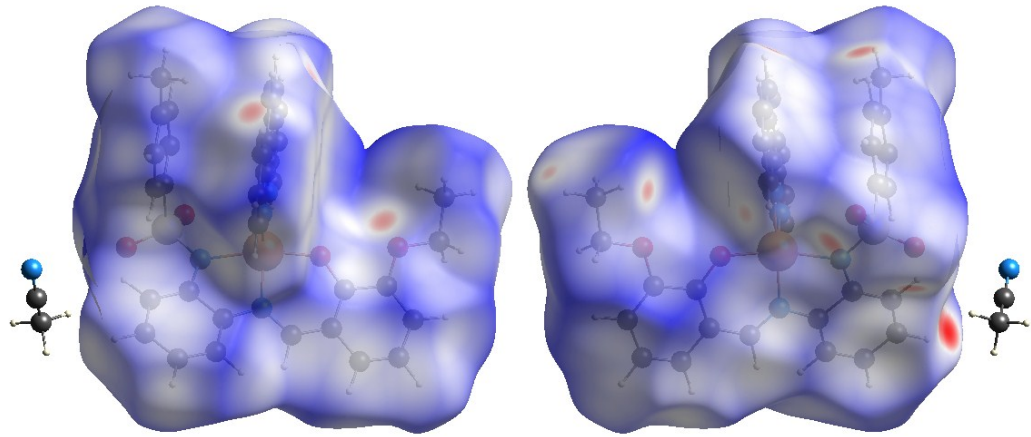


**Fig. S34** View of  $d_{\text{norm}}$  Hirschfeld surface analysis for  $[\text{CuL}^1(\text{phen})]$  (**4**).

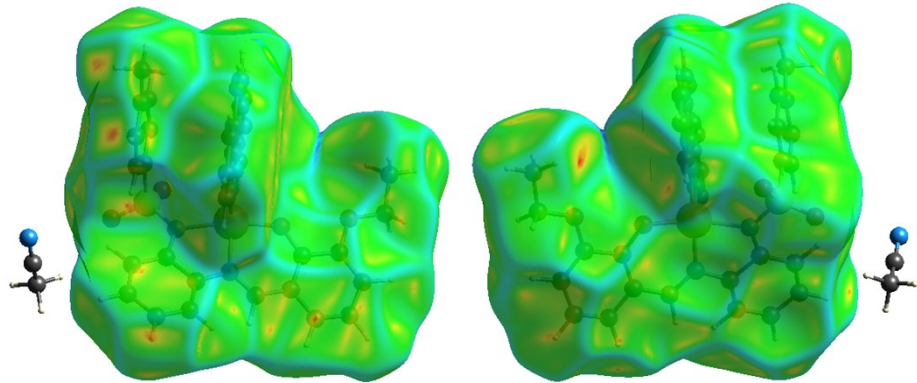


**Fig. S35** View of curvedness surface for  $[\text{CuL}^1(\text{phen})]$  (**4**).

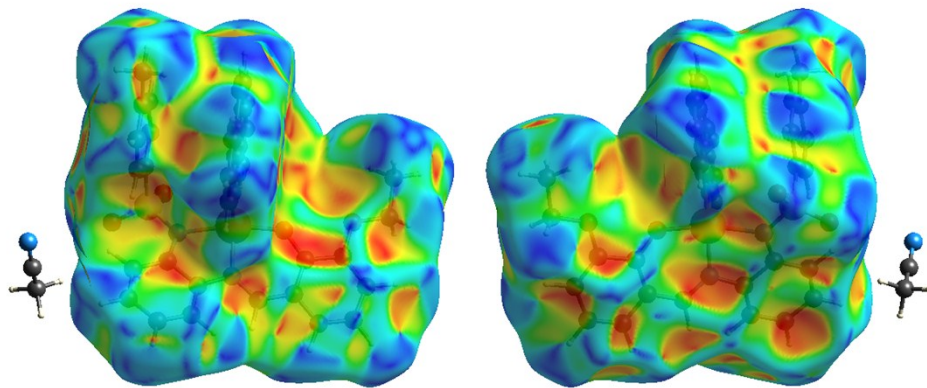


**Fig. S36** View of *shape index* surface for  $[\text{CuL}^1(\text{phen})]$  (**4**).

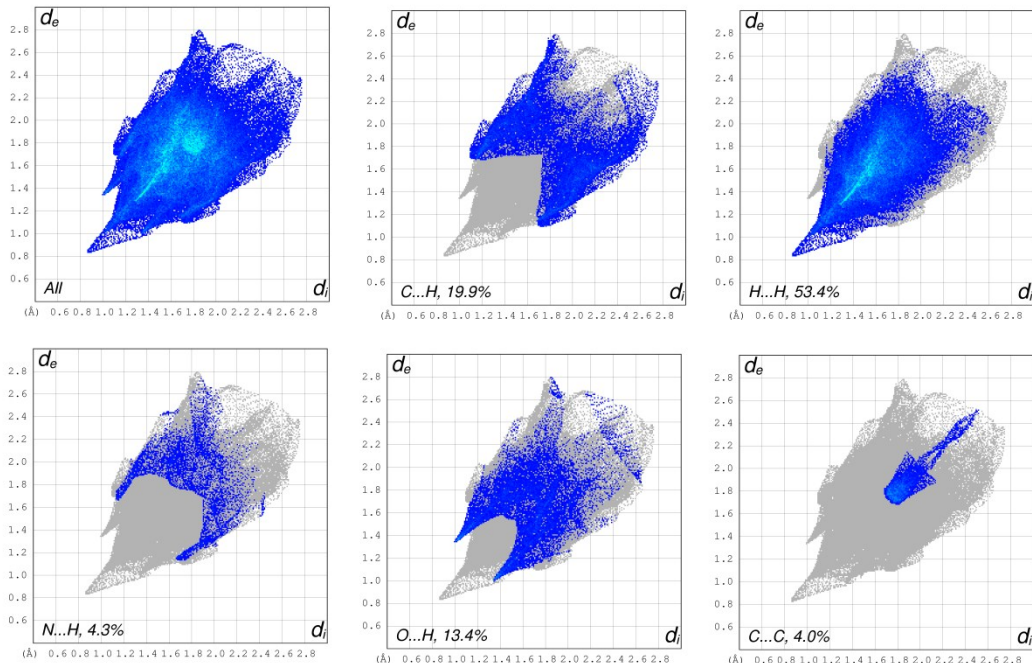


**Fig. S37** 2D fingerprint for  $[\text{CuL}^1(\text{phen})]$  (**4**).

The plots of 2D fingerprint (Fig. S37) for  $[\text{CuL}^1(\text{phen})]$  (**4**) show the contribution of the different interactions. Noteworthy the asymmetrical H...H interaction, probably due the presence of the MeCN molecule in the crystal.

*Hirshfeld surface analysis of  $[\text{CuL}^2(2,2'\text{-bpy})]$  (**6**).* Figure S38 shows the front and back surfaces modeled on  $d_{\text{norm}}$  for  $[\text{CuL}^2(2,2'\text{-bpy})]$  (**6**) and it evidence the red spots. These are

consequent with the above discussed for the supramolecular structure of this compound. In the right one are evident the red spots due the C-H...O interactions established by the the 2,2'-bpy ligand. Surfaces mapped with curvedness and shape index are drawn in Figures S39 and S40.

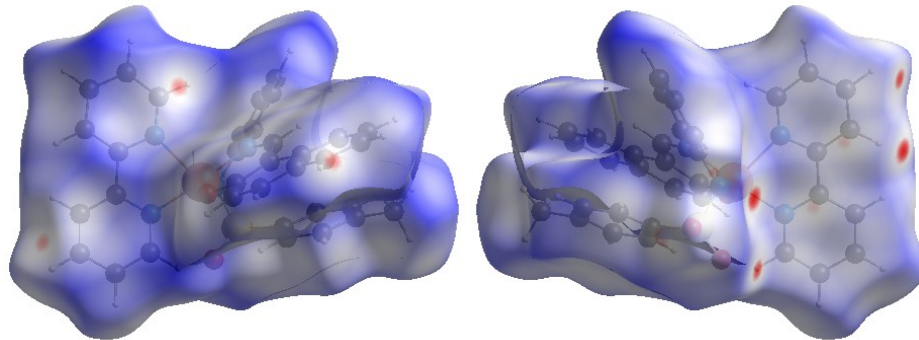


**Fig. S38** View of  $d_{\text{norm}}$  Hirschfeld surface analysis for  $[\text{CuL}^2(2,2'\text{-bpy})]$  (6).

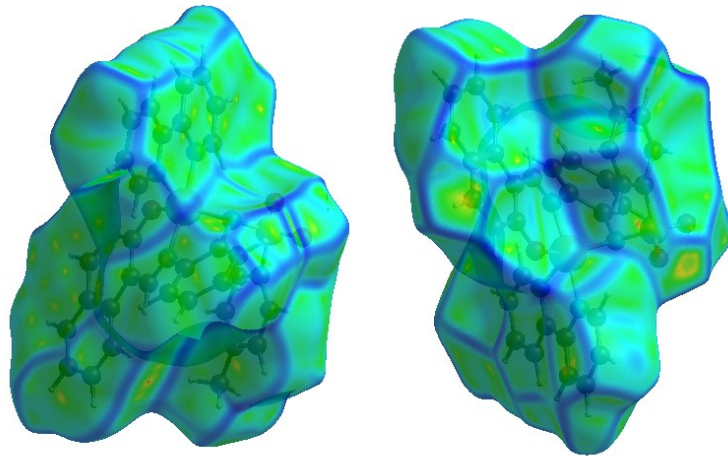


**Fig. S39** View of curvedness surface for  $[\text{CuL}^2(2,2'\text{-bpy})]$  (6).

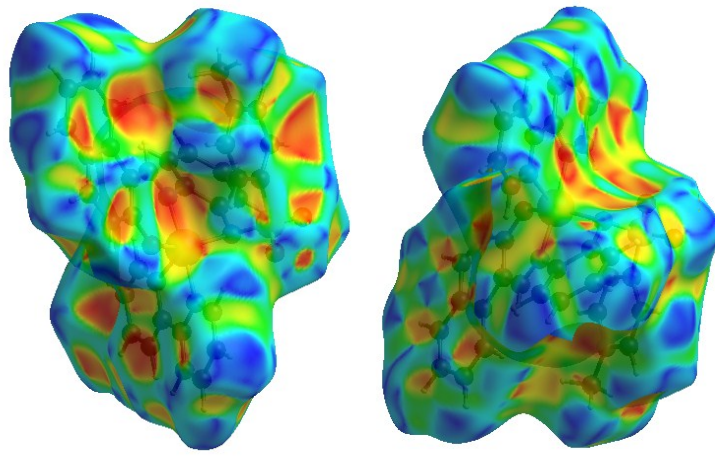


**Fig. S40** View of *shape index* surface for  $[\text{CuL}^2(2,2'\text{-bpy})]$  (6).

The plots of 2D fingerprint (Fig. S41) for  $[\text{CuL}^2(2,2'\text{-bpy})]$  (6) show the contribution of the different interactions. The importance of the O...H interactions, with the classical spikes in the left bottom of the fingerprint<sup>10</sup> is due to abovementioned C-H...O interactions above discussed. Among the C...C interactions (7.0 %) are the  $\pi,\pi$ -staking ones also abovementioned.

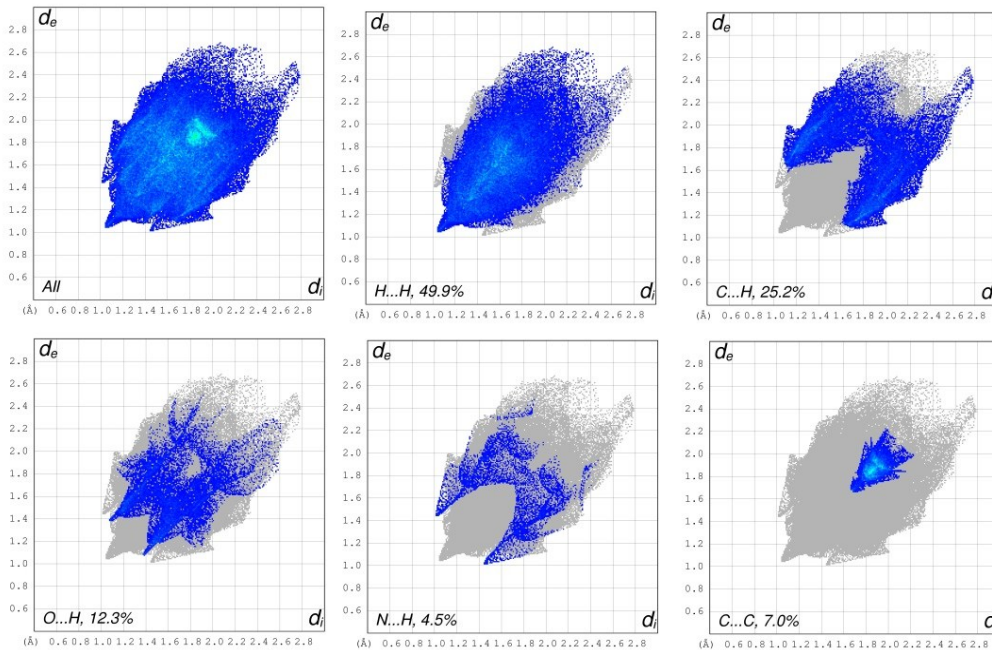


**Fig. S41** 2D fingerprint for  $[\text{CuL}^2(2,2'\text{-bpy})]$  (6).

*Hirshfeld surface analysis of  $[Cu_2L^2_2(4,4'-bpy)_3]$  (7).* For this purpose, also the whole molecule was studied, the dimer of formula  $[Cu_2L^2_2(4,4'-bpy)_3]$  (note that the asymmetric unit contains a half of it). Figure S42 shows the front and back surfaces modelled on  $d_{norm}$ . Red spots correspond with abovementioned interactions, especially noticeable are those C-H...O with the sulfonyl oxygen atoms or that formed with the free end of the monodentated 4,4'-bipyridine ligand (in the right bottom corner). Surfaces mapped with curvedness and shape index are drawn in Figures S43 and S44. Figure S45 shows the 2D fingerprint obtained for this compound. Again, percentages of the contributions are given in the fingerprint.

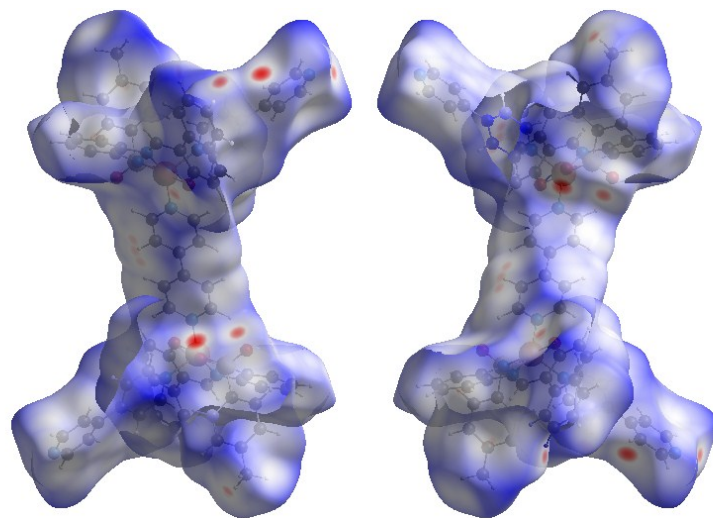


**Fig. S42** View of  $d_{norm}$  Hirshfeld surface analysis for  $[Cu_2L^2_2(4,4'-bpy)_3]$  (7).

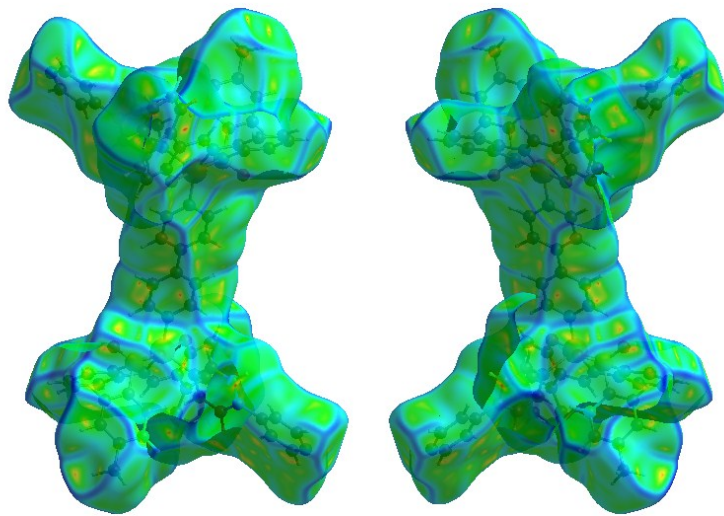


**Fig. S43** View of curvedness surface for  $[\text{Cu}_2\text{L}^1_2(4,4'\text{-bpy})_3]$  (7).

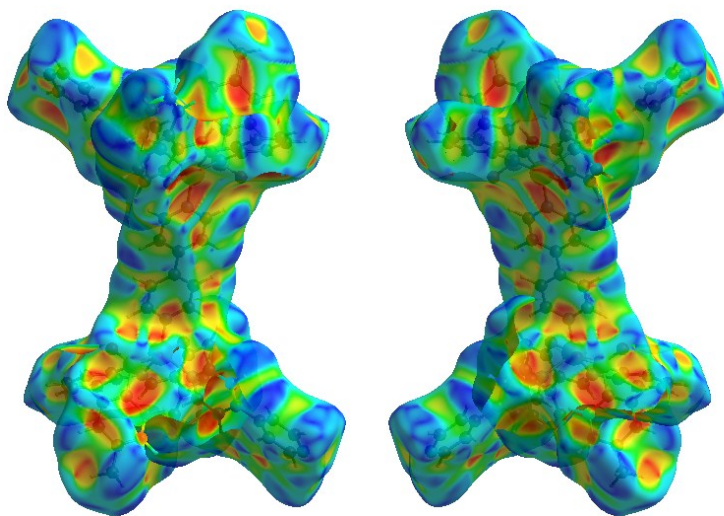


**Fig. S44** View of *shape index* surface for  $[\text{Cu}_2\text{L}^1_2(4,4'\text{-bpy})_3]$  (7).

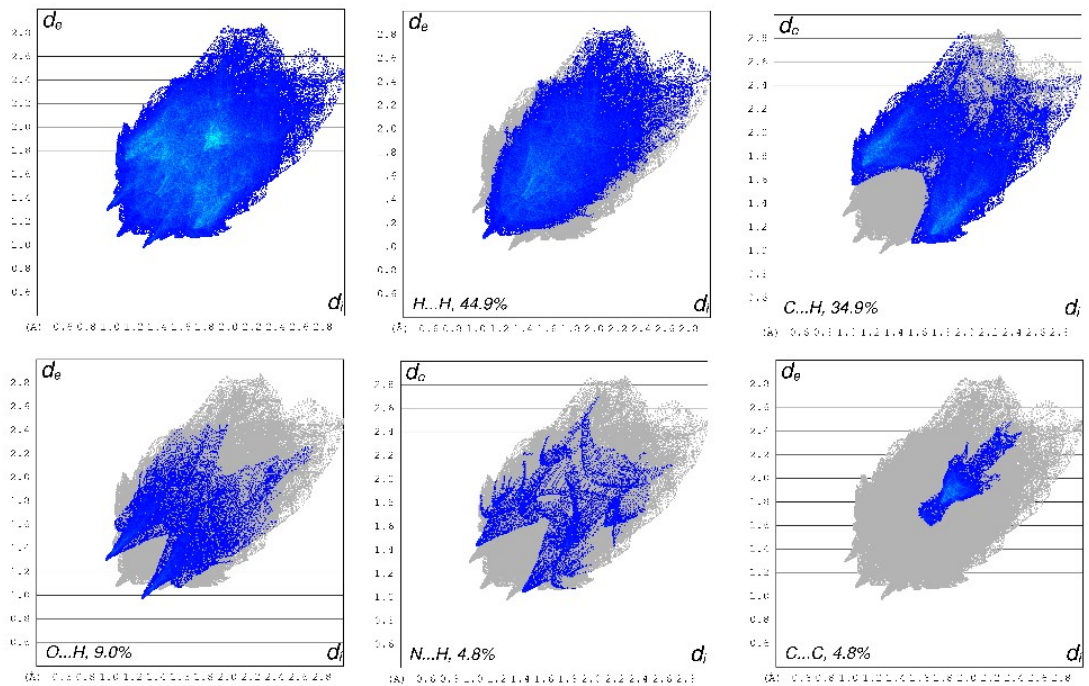


**Fig. S45** 2D fingerprint for for  $[\text{Cu}_2\text{L}^2(4,4'\text{-bpy})_3]$  (7).

**DFT calculations.**

**Table S12.** Selected Bond Lengths ( $\text{\AA}$ ) and angles ( $^\circ$ ) for the triclinic (**1a**) and orthorhombic (**1b**) forms of  $[\text{CuL}^1(\text{H}_2\text{O})]\cdot\text{H}_2\text{O}$  and the DFT calculated geometry.

	Triclinic $[\text{CuL}^1(\text{H}_2\text{O})]\cdot\text{H}_2\text{O}$ ( <b>1a</b> )	Orthorhombic $[\text{CuL}^1(\text{H}_2\text{O})]\cdot\text{H}_2\text{O}$ ( <b>1b</b> )	DFT $[\text{CuL}^1(\text{H}_2\text{O})]\cdot\text{H}_2\text{O}$
Cu-O(1)	1.8994(15)	1.893(3)	1.916
Cu-N(1)	1.9222(18)	1.923(3)	1.947
Cu-O(1W)	1.936(2)	1.953(3)	1.986
Cu-N(2)	2.0039(18)	1.988(3)	1.995
Cu-O(4 <sup>i</sup> )	2.7566(18)		
O(1)-Cu-N(1)	93.98(7)	95.00(11)	94.17
O(1)-Cu-O(1W)	84.04(8)	85.75(12)	86.80
N(1)-Cu-O(1W)	174.06(9)	168.88(14)	168.20
O(1)-Cu-N(2)	175.48(7)	174.04(14)	170.60
N(1)-Cu-N(2)	83.56(7)	83.86(12)	83.23
O(1W)-Cu-N(2)	98.04(9)	96.50(12)	97.60

**Table S13.** Selected Bond Lengths ( $\text{\AA}$ ) and angles ( $^\circ$ ) for **4** and **6** complexes and corresponding calculated geometries.

	$[\text{CuL}^1(\text{phen})]$ ( <b>4</b> )	$[\text{CuL}^1(\text{phen})]$ (DFT)	$[\text{CuL}^2(2,2'\text{-bpy})]$ ( <b>6</b> )	$[\text{CuL}^2(2,2'\text{-bpy})]$ (DFT)
Cu-O(13)	1.933(2)	1.960	1.9292(16)	1.956
Cu-N(11)	2.036(2)	2.046	2.043(2)	2.046
Cu-N(12)	1.951(2)	1.958	1.9373(19)	1.972
Cu-N(21)	1.999(2)	2.044	2.0130(19)	2.054
Cu-N(22)	2.318(3)	2.288	2.2499(19)	2.319
O(13)-Cu-N(11)	159.53(9)	157.27	154.31(7)	156.15
O(13)-Cu-N(12)	92.44(10)	90.63	91.01(8)	91.92
O(13)-Cu-N(21)	85.98(9)	88.00	87.20(7)	86.25
O(13)-Cu-N(22)	107.72(9)	107.52	112.51(7)	103.83
N(12)-Cu-N(21)	177.14(11)	175.15	174.40(8)	173.04
N(12)-Cu-N(11)	81.55(10)	82.58	82.61(8)	81.13
N(21)-Cu-N(11)	100.73(10)	100.41	101.23(8)	103.14
N(12)-Cu-N(22)	101.35(10)	99.88	98.12(8)	97.33
N(21)-Cu-N(22)	76.90(10)	76.13	77.71(7)	76.64
N(11)-Cu-N(22)	92.67(9)	95.04	93.06(7)	99.69

**Table S14.** Optimized Cartesian coordinates ( $\text{\AA}$ ) for  $[\text{CuL}^1(\text{H}_2\text{O})]\cdot\text{H}_2\text{O}$ .

$[\text{CuL}^1(\text{H}_2\text{O})]\cdot\text{H}_2\text{O}$ , TPSSh/TZVP, acetonitrile (IEFPM), 0 imaginary frequencies

Center Number	Atomic Number	Coordinates (Angstroms)		
		X	Y	Z
1	8	-2.618306	-3.215196	-0.737071
2	1	-3.192337	-2.680352	-0.201413
3	1	-2.878104	-4.115287	-0.579462
4	29	-0.581404	-0.108532	-0.222023
5	16	2.399812	-0.556453	-1.352515
6	7	-0.773910	1.791024	0.006749
7	8	-2.424164	-0.487606	-0.009731
8	8	-4.822991	-1.481843	0.195422
9	8	1.759138	-1.833192	-1.646849
10	8	3.025852	0.080599	-2.478004
11	8	-0.316791	-2.038212	-0.082280
12	1	0.255783	-2.455059	-0.483316
13	1	-1.074424	-2.532495	-0.234403
14	7	1.308174	0.347988	-0.638176
15	6	-3.361622	0.361645	0.268816
16	6	-4.701738	-0.127780	0.414687
17	6	-5.732858	0.702139	0.740911
18	1	-6.593674	0.360345	0.827537
19	6	-5.497583	2.067232	0.945601
20	1	-6.201779	2.626582	1.183740
21	6	-4.251075	2.580257	0.798981
22	1	-4.109212	3.489126	0.933859
23	6	-3.165633	1.749263	0.444147
24	6	-6.129913	-2.053780	0.324954
25	1	-6.748593	-1.612282	-0.276315
26	1	-6.453188	-1.946682	1.232543
27	6	-6.030727	-3.496633	-0.016592
28	1	-6.909280	-3.882956	-0.023232
29	1	-5.488549	-3.943198	0.638156
30	1	-5.630783	-3.593391	-0.882877
31	6	-1.897870	2.371335	0.289207
32	1	-1.871360	3.293235	0.402036
33	6	0.450985	2.504487	-0.105475
34	6	0.587190	3.872697	0.119314
35	1	-0.155222	4.376609	0.361054
36	6	1.809576	4.478616	-0.013832
37	1	1.891078	5.396176	0.113650
38	6	2.917151	3.723944	-0.335957
39	1	3.748106	4.135106	-0.408691

40	6	2.802347	2.356195	-0.554596
41	1	3.556340	1.857297	-0.776033
42	6	1.570071	1.731091	-0.442167
43	6	3.666386	-0.905260	-0.173589
44	6	4.884955	-1.377671	-0.656568
45	1	5.025951	-1.456154	-1.572095
46	6	5.872977	-1.723308	0.223586
47	1	6.675287	-2.061740	-0.102601
48	6	5.701902	-1.583256	1.579438
49	6	4.496190	-1.083304	2.053687
50	1	4.367155	-0.973993	2.968912
51	6	3.479170	-0.746221	1.165954
52	1	2.673116	-0.412057	1.486423
53	6	6.831753	-1.910069	2.547306
54	1	6.462781	-2.243312	3.368418
55	1	7.341431	-1.117467	2.724733
56	1	7.401642	-2.576586	2.159507

$$E(UTPSSh) = -3452.55783429 \text{ Hartree}$$

$$\text{Zero-point correction} = 0.427865$$

$$\text{Thermal correction to Energy} = 0.460596$$

$$\text{Thermal correction to Enthalpy} = 0.461540$$

$$\text{Thermal correction to Gibbs Free Energy} = 0.360908$$

$$\text{Sum of electronic and zero-point Energies} = -3452.548153$$

$$\text{Sum of electronic and thermal Energies} = -3452.515422$$

$$\text{Sum of electronic and thermal Enthalpies} = -3452.514478$$

$$\text{Sum of electronic and thermal Free Energies} = -3452.615111$$

**Table S15.** Optimized Cartesian coordinates ( $\text{\AA}$ ) for  $[\text{CuL}^2(2,2'\text{-bpy})]$ .

$[\text{CuL}^2(2,2'\text{-bpy})]$ , TPSSh/TZVP, acetonitrile (IEFPM), 0 imaginary frequencies

Center Number	Atomic Number	Coordinates (Angstroms)		
		X	Y	Z
1	29	-0.710226	-0.624752	-0.229521
2	16	-1.928208	2.374177	-0.554786
3	8	-2.847105	3.346331	0.108400
4	8	-2.391488	1.778684	-1.836502
5	8	0.535569	-1.773954	-1.213297
6	7	-1.538221	1.121892	0.440000
7	7	0.700934	-0.146642	1.041528
8	6	-0.406521	3.289297	-0.904281
9	6	0.488407	2.788413	-1.849406
10	1	0.256097	1.881059	-2.394040
11	6	1.672238	3.472613	-2.094974

12	1	2.364966	3.085192	-2.835186
13	6	1.985894	4.651121	-1.403533
14	6	1.074225	5.127379	-0.457376
15	1	1.297264	6.037559	0.089763
16	6	-0.119628	4.455324	-0.201868
17	1	-0.826579	4.837233	0.523708
18	6	3.262848	5.395786	-1.695437
19	1	4.106727	4.708490	-1.791712
20	1	3.488623	6.115640	-0.906991
21	1	3.181495	5.945958	-2.638509
22	6	-0.960171	1.440440	1.691510
23	6	-1.501781	2.332524	2.626643
24	1	-2.407241	2.867763	2.374174
25	6	-0.886359	2.525146	3.860213
26	1	-1.325005	3.215783	4.572054
27	6	0.263565	1.810963	4.196965
28	1	0.722165	1.935588	5.171235
29	6	0.809892	0.912777	3.287017
30	1	1.681801	0.331918	3.565711
31	6	0.222455	0.741753	2.029386
32	6	1.951726	-0.523404	1.005515
33	1	2.607692	-0.084834	1.752844
34	6	2.547781	-1.422115	0.080237
35	6	3.962070	-1.743058	0.213539
36	6	4.789699	-1.249845	1.252230
37	1	4.390005	-0.592599	2.013791
38	6	6.127272	-1.585877	1.336071
39	1	6.723404	-1.183744	2.148049
40	6	6.719825	-2.439821	0.390771
41	1	7.770069	-2.696733	0.466679
42	6	5.943355	-2.944725	-0.629364
43	1	6.372858	-3.610019	-1.371803
44	6	4.574297	-2.615900	-0.735582
45	6	3.783707	-3.153016	-1.795117
46	1	4.262521	-3.814929	-2.510445
47	6	2.462260	-2.860034	-1.917967
48	1	1.865415	-3.272039	-2.723558
49	6	1.792498	-1.987482	-0.993556
50	7	-2.188802	-1.278780	-1.479867
51	7	-1.992845	-1.976884	1.097986
52	6	-2.136561	-1.049342	-2.796900
53	1	-1.305302	-0.450765	-3.142943
54	6	-3.087997	-1.541289	-3.679195
55	1	-3.003824	-1.330246	-4.737245
56	6	-4.135877	-2.297853	-3.167373
57	1	-4.898344	-2.702409	-3.822076

58	6	-4.185696	-2.546893	-1.802409
59	1	-4.979310	-3.155773	-1.391742
60	6	-3.193506	-2.022733	-0.971786
61	6	-3.151430	-2.285633	0.486762
62	6	-4.229048	-2.830026	1.188901
63	1	-5.164250	-3.050267	0.691924
64	6	-4.089572	-3.077190	2.549274
65	1	-4.913893	-3.497998	3.112510
66	6	-2.884982	-2.772409	3.173753
67	1	-2.733908	-2.953311	4.230365
68	6	-1.867418	-2.216438	2.405899
69	1	-0.913630	-1.951850	2.848418

E(UTPSSh) = -3795.41995080 Hartree

Zero-point correction= 0.521370

Thermal correction to Energy= 0.558708

Thermal correction to Enthalpy= 0.559652

Thermal correction to Gibbs Free Energy= 0.447061

Sum of electronic and zero-point Energies= -3794.898581

Sum of electronic and thermal Energies= -3794.861243

Sum of electronic and thermal Enthalpies= -3794.860298

Sum of electronic and thermal Free Energies= -3794.972890

**Table S16.** Optimized Cartesian coordinates (Å) for [CuL<sup>1</sup>(phen)].

[CuL<sup>1</sup>(phen)], TPSSh/TZVP, acetonitrile (IEFPM), 0 imaginary frequencies

Center Number	Atomic Number	Coordinates (Angstroms)		
		X	Y	Z
1	29	0.660988	-0.429327	-0.293955
2	16	-2.174868	-0.917515	-1.967802
3	8	-1.543260	0.179621	-2.750471
4	8	-2.601575	-2.122643	-2.737665
5	7	-1.139894	-1.285416	-0.753097
6	7	1.031616	-2.265828	0.321425
7	8	2.567195	-0.046889	-0.510377
8	8	4.944491	0.990457	-0.877414
9	6	4.902545	-0.299946	-0.431533
10	6	6.016147	-1.078086	-0.177237
11	1	7.008075	-0.669545	-0.323886
12	6	5.883961	-2.407607	0.277198
13	1	6.773478	-2.995482	0.469413
14	6	4.634051	-2.938986	0.468817
15	1	4.514621	-3.959483	0.818097

16	6	3.466426	-2.166401	0.223756
17	6	3.573218	-0.819666	-0.241617
18	6	2.209867	-2.802880	0.451033
19	1	2.267361	-3.849118	0.755558
20	6	-0.154006	-2.985879	0.589828
21	6	-0.221753	-4.110619	1.415594
22	1	0.670017	-4.471485	1.915043
23	6	-1.434200	-4.760337	1.618702
24	1	-1.480935	-5.628640	2.265487
25	6	-2.585973	-4.270924	1.003062
26	1	-3.538274	-4.765545	1.160001
27	6	-2.536175	-3.134060	0.202752
28	1	-3.446109	-2.764169	-0.251272
29	6	-1.323274	-2.461715	-0.013556
30	6	-3.679100	-0.239212	-1.222084
31	6	-4.904741	-0.458454	-1.844906
32	1	-4.960473	-1.075750	-2.733232
33	6	-6.053580	0.109255	-1.301298
34	1	-7.010211	-0.066976	-1.782261
35	6	-5.996992	0.896441	-0.146034
36	6	-4.751686	1.092823	0.463559
37	1	-4.686565	1.686830	1.369408
38	6	-3.594310	0.533260	-0.066940
39	1	-2.637565	0.680326	0.418963
40	6	-7.241147	1.529780	0.420406
41	1	-8.134349	0.972690	0.131881
42	1	-7.353909	2.553288	0.047575
43	1	-7.197569	1.581223	1.510321
44	6	6.238724	1.574969	-1.103612
45	1	6.782074	0.978403	-1.845166
46	1	6.809517	1.567794	-0.168123
47	6	6.020889	2.989871	-1.597236
48	1	5.454018	2.992563	-2.530557
49	1	6.988065	3.464358	-1.779462
50	1	5.480692	3.581345	-0.855110
51	7	0.353013	1.557926	-0.710165
52	7	0.145200	0.477917	1.776478
53	6	0.523390	2.079678	-1.918589
54	1	0.747505	1.384086	-2.714996
55	6	0.405188	3.452984	-2.172277
56	1	0.554499	3.822005	-3.178669
57	6	0.092434	4.302235	-1.134389
58	1	-0.015904	5.368311	-1.299344
59	6	-0.081668	3.777797	0.162328
60	6	0.070064	2.381027	0.331108
61	6	-0.051575	1.809834	1.648256

62	6	-0.363890	2.648599	2.745071
63	6	-0.472340	2.039520	4.012545
64	1	-0.709379	2.646360	4.879346
65	6	-0.271641	0.681837	4.131336
66	1	-0.345712	0.183680	5.089753
67	6	0.039256	-0.063028	2.981740
68	1	0.207897	-1.132410	3.046860
69	6	-0.399852	4.595287	1.294628
70	1	-0.521841	5.661457	1.140365
71	6	-0.537684	4.054002	2.534800
72	1	-0.777588	4.679644	3.387184

$$E(\text{UTPSSh}) = -3871.87751286 \text{ Hartree}$$

$$\text{Zero-point correction} = 0.547364$$

$$\text{Thermal correction to Energy} = 0.586894$$

$$\text{Thermal correction to Enthalpy} = 0.587839$$

$$\text{Thermal correction to Gibbs Free Energy} = 0.469943$$

$$\text{Sum of electronic and zero-point Energies} = -3871.330149$$

$$\text{Sum of electronic and thermal Energies} = -3871.290619$$

$$\text{Sum of electronic and thermal Enthalpies} = -3871.289674$$

$$\text{Sum of electronic and thermal Free Energies} = -3871.407570$$

**Table S17.** Optimized Cartesian coordinates (Å) for [CuL<sup>1</sup>(4,4'-bpy)].

[CuL<sup>1</sup>(4,4'-bpy)], TPSSh/TZVP, acetonitrile (IEFPM), 0 imaginary frequencies

Center Number	Atomic Number	Coordinates (Angstroms)		
		X	Y	Z
1	7	3.355340	7.327865	1.023879
2	6	2.743468	6.992350	-0.119972
3	1	2.802426	7.718071	-0.925161
4	6	2.065725	5.794202	-0.311940
5	1	1.609779	5.583235	-1.271727
6	6	2.009651	4.868179	0.735208
7	6	2.648635	5.211866	1.931345
8	1	2.626792	4.550442	2.789106
9	6	3.297027	6.437871	2.023724
10	1	3.790899	6.722880	2.947499
11	7	-0.036370	1.137787	0.284335
12	6	1.072735	1.226390	1.037597
13	1	1.409107	0.304459	1.494851
14	6	1.758837	2.416392	1.214581
15	1	2.654015	2.423834	1.823359
16	6	1.301943	3.578374	0.582260
17	6	0.147064	3.470905	-0.200817

18	1	-0.272244	4.334584	-0.700991
19	6	-0.492451	2.248002	-0.319308
20	1	-1.404683	2.131365	-0.889469
21	29	-1.011205	-0.639598	0.136870
22	16	1.297379	-1.977658	-1.397098
23	8	1.001187	-0.690435	-2.086738
24	8	0.930714	-3.242768	-2.094912
25	7	-1.928504	-2.233259	0.813639
26	7	0.577041	-1.846843	0.088904
27	8	-2.647139	0.277840	-0.253016
28	6	-3.861269	-0.162146	-0.092595
29	6	-4.945063	0.702752	-0.468714
30	6	-6.259131	0.294614	-0.333636
31	1	-7.065126	0.957000	-0.622630
32	6	-6.572228	-0.980489	0.181329
33	6	-5.563460	-1.832942	0.551409
34	6	-4.200647	-1.448062	0.427265
35	6	-3.219762	-2.400262	0.836277
36	1	-3.614826	-3.354223	1.187880
37	6	-1.017430	-3.226237	1.241534
38	6	-1.345873	-4.317601	2.051595
39	1	-2.357018	-4.442785	2.420589
40	6	-0.368795	-5.241915	2.401713
41	1	-0.628272	-6.085134	3.031184
42	6	0.943721	-5.070085	1.959156
43	1	1.709414	-5.784886	2.238900
44	6	1.286027	-3.967091	1.183912
45	1	2.312865	-3.821990	0.871727
46	6	0.314801	-3.030241	0.815429
47	6	3.087229	-2.042681	-1.158918
48	6	3.764099	-0.914501	-0.697378
49	1	3.224288	-0.001135	-0.480637
50	6	5.141354	-0.972286	-0.527694
51	1	5.668153	-0.094568	-0.167596
52	6	5.860325	-2.141180	-0.815555
53	6	5.156302	-3.254542	-1.282452
54	1	5.692496	-4.168859	-1.513935
55	6	3.774910	-3.213683	-1.458290
56	1	3.235279	-4.077981	-1.824755
57	6	7.356722	-2.183009	-0.647565
58	1	7.661004	-1.709462	0.288815
59	1	7.725795	-3.209746	-0.655006
60	1	7.850277	-1.642446	-1.461647
61	1	-5.788369	-2.816883	0.949372
62	1	-7.610424	-1.274109	0.278686
63	8	-4.553677	1.914143	-0.959510

64	6	-5.584623	2.831219	-1.368954
65	1	-6.192786	2.365786	-2.152480
66	1	-6.231886	3.054755	-0.513511
67	6	-4.905373	4.084470	-1.879372
68	1	-4.299012	4.544387	-1.096226
69	1	-4.265465	3.858873	-2.734888
70	1	-5.663645	4.804523	-2.195923

E(UTPSSh) = -3795.6089742 Hartree

Zero-point correction= 0.535935

Thermal correction to Energy= 0.574592

Thermal correction to Enthalpy= 0.575536

Thermal correction to Gibbs Free Energy= 0.458296

Sum of electronic and zero-point Energies= -3795.073040

Sum of electronic and thermal Energies= -3795.034382

Sum of electronic and thermal Enthalpies= -3795.033438

Sum of electronic and thermal Free Energies= -3795.150678

**Table S18.** Optimized Cartesian coordinates (Å) for [CuL<sup>1</sup>(4,4'-bpy)<sub>2</sub>].

[CuL<sup>1</sup>(4,4'-bpy)<sub>2</sub>], TPSSh/TZVP, acetonitrile (IEFPM), 0 imaginary frequencies

Center Number	Atomic Number	Coordinates (Angstroms)		
		X	Y	Z
1	7	-8.518760	0.773476	-3.044447
2	6	-7.576241	-0.095400	-3.434826
3	1	-7.843582	-0.755043	-4.254602
4	6	-6.314687	-0.179528	-2.857594
5	1	-5.596719	-0.896265	-3.237676
6	6	-5.985891	0.686302	-1.809040
7	6	-6.965326	1.597343	-1.398691
8	1	-6.784256	2.283063	-0.579791
9	6	-8.199114	1.598951	-2.038561
10	1	-8.972094	2.294429	-1.726389
11	7	-2.138674	0.559129	0.073025
12	6	-2.792050	1.720887	-0.088428
13	1	-2.283943	2.606836	0.269987
14	6	-4.040278	1.803533	-0.683646
15	1	-4.510089	2.772890	-0.792209
16	6	-4.657550	0.641554	-1.159450
17	6	-3.968018	-0.563984	-0.989225
18	1	-4.395579	-1.504540	-1.313187
19	6	-2.730216	-0.564096	-0.365633
20	1	-2.191368	-1.483432	-0.180885
21	29	-0.315887	0.479066	1.089715

22	7	1.034741	-0.834498	-0.268448
23	7	4.663807	-5.775487	-3.879837
24	6	0.767014	-1.093176	-1.557669
25	1	-0.015489	-0.494634	-2.005850
26	6	1.448372	-2.049632	-2.297967
27	1	1.168068	-2.221094	-3.330042
28	6	2.470939	-2.789981	-1.695312
29	6	2.750352	-2.515662	-0.351907
30	1	3.543052	-3.034346	0.173038
31	6	2.015011	-1.544769	0.311774
32	1	2.220611	-1.318002	1.351610
33	6	3.226277	-3.816742	-2.446639
34	6	3.501522	-3.666836	-3.810351
35	1	3.185663	-2.782728	-4.351042
36	6	4.214721	-4.659965	-4.471219
37	1	4.441780	-4.554091	-5.527603
38	6	3.694504	-4.979014	-1.823803
39	1	3.499985	-5.169067	-0.775089
40	6	4.396656	-5.914712	-2.574099
41	1	4.759423	-6.824666	-2.106010
42	16	0.436688	2.969396	-0.915650
43	8	-0.209341	4.313959	-0.995158
44	8	-0.090631	1.939833	-1.849706
45	7	0.703006	0.874952	2.760175
46	7	0.359252	2.318467	0.593649
47	8	-0.981328	-1.187582	1.862403
48	6	-0.464894	-1.859191	2.844378
49	6	-0.911681	-3.209763	3.059463
50	6	-0.399200	-3.973456	4.091542
51	1	-0.739724	-4.991317	4.233882
52	6	0.566248	-3.445115	4.974711
53	6	1.008321	-2.157064	4.807685
54	6	0.510904	-1.346078	3.751937
55	6	0.990215	-0.003375	3.678680
56	1	1.658468	0.289879	4.489025
57	6	1.134658	2.217214	2.845900
58	6	1.663681	2.804341	3.999874
59	1	1.752065	2.228110	4.913000
60	6	2.066761	4.133789	3.997142
61	1	2.475400	4.576764	4.897809
62	6	1.914364	4.892587	2.837142
63	1	2.211688	5.935522	2.825762
64	6	1.356958	4.335514	1.691815
65	1	1.206483	4.953818	0.817554
66	6	0.950642	2.989402	1.670823
67	6	2.188917	3.225219	-1.290979

68	6	2.592275	4.404738	-1.907857
69	1	1.870202	5.187064	-2.106498
70	6	3.932396	4.566204	-2.249971
71	1	4.250764	5.488194	-2.725339
72	6	4.872939	3.565093	-1.986878
73	6	4.437335	2.390189	-1.359848
74	1	5.153256	1.606034	-1.136038
75	6	3.103052	2.211564	-1.014243
76	1	2.775339	1.301741	-0.526346
77	6	6.316079	3.736123	-2.383801
78	1	6.585297	4.791835	-2.449166
79	1	6.982903	3.248050	-1.670010
80	1	6.499345	3.285854	-3.365135
81	1	1.745069	-1.732918	5.482320
82	1	0.948539	-4.064243	5.777384
83	8	-1.849759	-3.642117	2.165748
84	6	-2.349513	-4.981962	2.320194
85	1	-1.519424	-5.691899	2.231796
86	1	-2.794410	-5.091024	3.315625
87	6	-3.380752	-5.213125	1.235477
88	1	-4.207956	-4.506471	1.329385
89	1	-2.933968	-5.103963	0.245017
90	1	-3.780427	-6.226117	1.323895

$$E(UTPSSh) = -4291.1863039 \text{ Hartree}$$

Zero-point correction= 0.694052

Thermal correction to Energy= 0.743619

Thermal correction to Enthalpy= 0.744563

Thermal correction to Gibbs Free Energy= 0.600744

Sum of electronic and zero-point Energies= -4290.492252

Sum of electronic and thermal Energies= -4290.442685

Sum of electronic and thermal Enthalpies= -4290.441741

Sum of electronic and thermal Free Energies= -4290.585560

**Table S19.** Optimized Cartesian coordinates (Å) for [CuL<sup>2</sup>(4,4'-bpy)].

[CuL<sup>2</sup>(4,4'-bpy)], TPSSh/TZVP, acetonitrile (IEFPM), 0 imaginary frequencies

Center Number	Atomic Number	Coordinates (Angstroms)		
		X	Y	Z
1	7	6.423202	5.665329	0.691971
2	6	5.207248	6.129839	0.374265
3	1	5.127630	7.202710	0.229113
4	6	4.083808	5.323553	0.233816
5	1	3.127493	5.771869	-0.007296

6	6	4.206165	3.944633	0.435597
7	6	5.472896	3.453938	0.769724
8	1	5.641985	2.394492	0.920044
9	6	6.534744	4.343664	0.881807
10	1	7.525675	3.978086	1.132535
11	7	0.835161	1.337675	0.053322
12	6	1.794980	1.091912	0.960856
13	1	1.657333	0.209671	1.573238
14	6	2.898533	1.914196	1.117913
15	1	3.626069	1.680514	1.884728
16	6	3.041888	3.042340	0.302106
17	6	2.037675	3.283249	-0.642223
18	1	2.096130	4.126360	-1.318720
19	6	0.958432	2.420174	-0.731686
20	1	0.157615	2.584965	-1.439711
21	29	-0.787371	0.122203	-0.062263
22	16	0.880591	-2.140803	-1.372453
23	8	1.231187	-0.890010	-2.101526
24	8	0.088648	-3.170337	-2.103934
25	7	-2.333579	-0.892147	0.558625
26	7	0.134660	-1.642465	0.018567
27	8	-1.878728	1.629681	-0.526754
28	6	-3.170782	1.747820	-0.464157
29	6	-3.712329	2.999383	-0.905942
30	1	-3.007512	3.746726	-1.250985
31	6	-5.051174	3.236271	-0.901552
32	1	-5.434311	4.192340	-1.244789
33	6	-5.983210	2.254437	-0.452661
34	6	-7.368528	2.528816	-0.462919
35	1	-7.699086	3.501018	-0.814411
36	6	-8.282254	1.589276	-0.038669
37	1	-9.344174	1.805825	-0.049355
38	6	-7.817033	0.340516	0.406368
39	1	-8.524468	-0.410649	0.740199
40	6	-6.466628	0.049882	0.426036
41	1	-6.170411	-0.930590	0.775797
42	6	-5.498195	0.990897	-0.000583
43	6	-4.063210	0.738058	0.005588
44	6	-3.582401	-0.511484	0.479731
45	1	-4.329418	-1.230117	0.803746
46	6	-1.964181	-2.160361	1.062025
47	6	-2.776957	-2.972563	1.859727
48	1	-3.761393	-2.636028	2.163486
49	6	-2.319123	-4.214438	2.284371
50	1	-2.954006	-4.837742	2.903282
51	6	-1.039679	-4.643231	1.929178

52	1	-0.676309	-5.608068	2.264726
53	6	-0.209245	-3.824567	1.170689
54	1	0.794134	-4.151135	0.926993
55	6	-0.654361	-2.573478	0.730344
56	6	2.437851	-2.938931	-0.920891
57	6	3.432909	-2.198338	-0.284600
58	1	3.272733	-1.153795	-0.048481
59	6	4.633386	-2.815244	0.041935
60	1	5.407044	-2.239752	0.539753
61	6	4.862212	-4.165102	-0.261408
62	6	3.848096	-4.881752	-0.902262
63	1	4.003198	-5.927533	-1.145982
64	6	2.637157	-4.278344	-1.235878
65	1	1.854450	-4.837978	-1.732559
66	6	6.177777	-4.815293	0.078641
67	1	6.495753	-4.555136	1.091148
68	1	6.112117	-5.901756	0.002911
69	1	6.962271	-4.477118	-0.605931

E(UTPSSh) = -3795.4102025 Hartree

Zero-point correction= 0.521411

Thermal correction to Energy= 0.559011

Thermal correction to Enthalpy= 0.559955

Thermal correction to Gibbs Free Energy= 0.443276

Sum of electronic and zero-point Energies= -3794.888791

Sum of electronic and thermal Energies= -3794.851191

Sum of electronic and thermal Enthalpies= -3794.850247

Sum of electronic and thermal Free Energies= -3794.966927

**Table S20.** Optimized Cartesian coordinates (Å) for [CuL<sup>2</sup>(4,4'-bpy)<sub>2</sub>].

[CuL<sup>2</sup>(4,4'-bpy)<sub>2</sub>], TPSSh/TZVP, acetonitrile (IEFPM), 0 imaginary frequencies

Center Number	Atomic Number	Coordinates (Angstroms)		
		X	Y	Z
1	7	9.023979	-2.153071	1.379235
2	6	8.077116	-3.100443	1.341425
3	1	8.396623	-4.106611	1.594747
4	6	6.752541	-2.857233	0.997852
5	1	6.045741	-3.677860	0.971007
6	6	6.362664	-1.555341	0.665334
7	6	7.347561	-0.562173	0.701763
8	1	7.110383	0.470439	0.475607
9	6	8.644755	-0.907805	1.061467
10	1	9.418295	-0.147115	1.101405

11	7	2.320179	-0.635893	-0.412220
12	6	3.350169	0.021322	-0.968838
13	1	3.092617	0.785696	-1.690882
14	6	4.671103	-0.251210	-0.653196
15	1	5.457999	0.296444	-1.156086
16	6	4.966576	-1.240666	0.291034
17	6	3.886300	-1.919865	0.865184
18	1	4.040213	-2.684362	1.616187
19	6	2.593642	-1.596411	0.485024
20	1	1.739334	-2.116114	0.897414
21	29	0.369607	-0.271162	-1.025670
22	7	-0.736740	-0.192880	1.038576
23	7	-4.060050	-0.924243	7.289562
24	6	-0.121916	0.099980	2.195606
25	1	0.891714	0.469926	2.109409
26	6	-0.731300	-0.032071	3.435653
27	1	-0.169244	0.204127	4.330934
28	6	-2.052068	-0.486444	3.511889
29	6	-2.692963	-0.786534	2.304542
30	1	-3.722641	-1.121808	2.284625
31	6	-2.004852	-0.628036	1.110260
32	1	-2.488442	-0.854812	0.167269
33	6	-2.742989	-0.637806	4.811453
34	6	-2.482299	0.227031	5.880148
35	1	-1.779846	1.045678	5.779321
36	6	-3.158377	0.044789	7.080639
37	1	-2.971439	0.712419	7.916118
38	6	-3.684850	-1.650490	5.023788
39	1	-3.921396	-2.366783	4.246148
40	6	-4.305455	-1.750426	6.263404
41	1	-5.033129	-2.535470	6.444907
42	16	1.252076	2.864411	-0.514397
43	8	2.291078	3.656725	-1.238537
44	8	1.701949	2.198262	0.736672
45	7	-1.010454	-0.144213	-2.443364
46	7	0.573398	1.696894	-1.453210
47	8	0.142738	-2.220145	-1.017768
48	6	-0.888813	-2.899645	-1.403535
49	6	-0.904713	-4.297516	-1.073942
50	1	-0.048718	-4.686834	-0.534939
51	6	-1.955046	-5.096161	-1.405340
52	1	-1.942481	-6.147977	-1.135950
53	6	-3.094721	-4.587078	-2.097177
54	6	-4.188865	-5.426834	-2.399661
55	1	-4.135479	-6.470928	-2.107523
56	6	-5.303919	-4.937029	-3.045270

57	1	-6.140469	-5.587405	-3.273390
58	6	-5.348810	-3.576024	-3.392232
59	1	-6.228278	-3.173715	-3.883191
60	6	-4.291032	-2.734633	-3.105027
61	1	-4.387919	-1.688259	-3.366827
62	6	-3.120848	-3.208879	-2.464306
63	6	-1.978027	-2.366075	-2.155490
64	6	-1.914663	-1.054352	-2.698493
65	1	-2.681944	-0.797849	-3.424369
66	6	-0.950555	1.062940	-3.172583
67	6	-1.619319	1.293340	-4.379667
68	1	-2.216313	0.509749	-4.830750
69	6	-1.513189	2.519172	-5.025682
70	1	-2.037620	2.684657	-5.959554
71	6	-0.706833	3.515184	-4.476809
72	1	-0.604127	4.471254	-4.978404
73	6	-0.001287	3.288645	-3.299745
74	1	0.656189	4.056839	-2.916246
75	6	-0.101835	2.059103	-2.626561
76	6	-0.069001	4.025475	-0.086817
77	6	0.171197	5.393999	-0.145261
78	1	1.125516	5.761793	-0.501459
79	6	-0.833838	6.275237	0.245319
80	1	-0.650957	7.343614	0.195008
81	6	-2.073220	5.807537	0.694402
82	6	-2.287717	4.423547	0.735601
83	1	-3.246758	4.040481	1.068839
84	6	-1.294427	3.530184	0.352314
85	1	-1.470279	2.461678	0.382091
86	6	-3.146124	6.765921	1.141502
87	1	-3.038000	7.736274	0.653517
88	1	-4.141629	6.373477	0.924394
89	1	-3.086169	6.930252	2.222589

---

E(UTPSSh) = -4290.9885268 Hartree

Zero-point correction=	0.680308
Thermal correction to Energy=	0.728498
Thermal correction to Enthalpy=	0.729442
Thermal correction to Gibbs Free Energy=	0.589065
Sum of electronic and zero-point Energies=	-4290.308219
Sum of electronic and thermal Energies=	-4290.260029
Sum of electronic and thermal Enthalpies=	-4290.259084
Sum of electronic and thermal Free Energies=	-4290.399462

## References

- 1 P. C. Brown, R. L. Towns and L. M. Trefonas, *J. Amer. Chem. Soc.*, 1970, **92**, 7436-7440.
- 2 G. Bertier and J. Serre, in "*The Chemistry of the Carbonyl Group*", Ed. S. Patai. Interscience, New York, 1966.
- 3 P. Adao, J. C. Pessoa, R. T. Henriques, M. L. Kuznetsov, F. Avecilla, M. R. Maurya, U. Kumar and I. Correia, *Inorg. Chem.*, 2009, **48**, 3542-3561.
- 4 B. S. Creaven, E. Czegledi, M. Devereux, E. A. Enyedy, A. F.-A. Kia, D. Karcz, A. Kellett, S. McClean, N. V. Nagy, A. Noble, A. Rockenbauer, T. Szabo-Planka and M. Walsh, *Dalton Trans.* 2010, **39**, 10854-10865.
- 5 H. Petek, C. Albayrak, M. Odabasoglu, I. Senel and O. Buyukgungor, *Struct. Chem.*, 2010, **21**, 681-690.
- 6 CrystalExplorer (Version 3.1), S. K. Wolff, D. J. Grimwood, J. J. McKinnon, M. J. Turner, D. Jayatilaka and M. A. Spackman, University of Western Australia, Perth, Australia. [www.hirshfeldsurface.net](http://www.hirshfeldsurface.net)
- 7 J. J. MacKinnon, M. A. Spackman and A. S. Mitchell, *Acta Crystallogr.*, 2004, **B60**, 627-668; M. A. Spackman and D. Jayatilaka, *CrystEngComm.*, 2009, **11**, 19-32.
- 8 J. J. McKinnon, D. Jayatilaka and M. A. Spackman, *Chem. Commun.*, 2007, 3814-3816.
- 9 M. A. Spackman and J. J. MacKinnon, *CrystEngComm.*, 2002, **4**, 378-392; J. J. MacKinnon, D. Jayatilaka and M. A. Spackman, *Chem. Commun.* 2007, 3814-3816; H. F. Clausen, M. S. Chevallier, M. A. Spackman and B. B. Iversen, *New J. Chem.*, 2010, **34**, 193-199.